Journal of Chromatography A, 1357 (2014) 36–52

Contents lists available at ScienceDirect

Journal of Chromatography A

journal homepage: www.elsevier.com/locate/chroma

Review

Core–shell particles: Preparation, fundamentals and applications in high performance liquid chromatography

Richard Hayes[a], Adham Ahmed[a], Tony Edge[b], Haifei Zhang[a,*]

[a] Department of Chemistry, University of Liverpool, Liverpool L69 7ZD, UK
[b] Thermo Fisher Scientific, Runcorn WA7 1TA, UK

ARTICLE INFO

Article history:
Received 31 March 2014
Received in revised form 1 May 2014
Accepted 2 May 2014
Available online 9 May 2014

Keywords:
Core–shell particles
Fused-core microspheres
Preparation methods
HPLC
Fast separation

ABSTRACT

The challenges in HPLC are fast and efficient separation for a wide range of samples. Fast separation often results in very high operating pressure, which places a huge burden on HPLC instrumentation. In recent years, core–shell silica microspheres (with a solid core and a porous shell, also known as fused-core or superficially porous microspheres) have been widely investigated and used for highly efficient and fast separation with reasonably low pressure for separation of small molecules, large molecules and complex samples. In this review, we firstly show the types of core–shell particles and how they are generally prepared, focusing on the methods used to produce core–shell silica particles for chromatographic applications. The fundamentals are discussed on why core–shell particles can perform better with low back pressure, in terms of van Deemter equation and kinetic plots. The core–shell particles are compared with totally porous silica particles and also monolithic columns. The use of columns packed with core–shell particles in different types of liquid chromatography is then discussed, followed by illustrating example applications of such columns for separation of various types of samples. The review is completed with conclusion and a brief perspective on future development of core–shell particles in chromatography.

Contents

* Corresponding author. Tel.: +44 151 7943545; fax: +44 151 7943588.
E-mail address: zhanghf@liv.ac.uk (H. Zhang).

http://dx.doi.org/10.1016/j.chroma.2014.05.010

1. Introduction

Among different types of chromatography, high performance liquid chromatography (HPLC) has been most widely used as an essential analysis tool for research, manufacturing, clinical tests, and diagnostics. This is due to its universal applicability and remarkable assay precision [1]. Two types of columns, i.e., packed column and monolithic column, have been used as stationary phases for routine HPLC. Silica microspheres are the mostly used packing materials for packed columns. While for monolithic columns, both porous silica and crosslinked polymers are frequently used. The challenges in HPLC are highly efficient and fast separation with high resolution and ideally low back pressure for various types of samples, e.g., in pharmaceuticals, food, life science, environmental and also the daily analysis in research labs [2].

Porous monoliths containing highly interconnected pores are widely used as monolithic columns for fast separation with low back pressure [3,4]. The large pores are in the category of macropores (>50 nm, around 1 μm for polymer monolith). For silica monoliths, in addition to the macropores, mesopores (2–50 nm) are present in the silica wall. The highly interconnected porosity results into high permeability and hence low back pressure even at high flow rates. Satisfying performance has been achieved particularly for large biomolecules [5,6]. The main obstacles for the wider use of monolithic columns are the reproducibility of the pore structures and the delicate cladding procedure to fit the monolith into a column. As a result, the analysis performance of monolithic columns may vary from batch to batch. Furthermore, the mechanical stability is generally weak for monolithic columns. There is an additional issue with polymer monoliths, i.e., the potential swelling problems in the presence of solvents.

Packed columns with silica microspheres are still dominating the market and most widely used. Although various polymer and ceramic microspheres have been used as packing materials, silica microspheres are the mostly investigated and used materials. Both nonporous and porous silica microspheres have been used. For small nonporous particles, the separation occurs on the particle surface and band-broadening is alleviated because of the short diffusion path, thus allowing faster mass transfer [7]. However, due to the low surface area, retention, selectivity and therefore resolution are limited. The loading capacity is also a critical issue. For porous silica microspheres, in addition to the particle surface, the pore surface provides more sites to interact with analytes. For liquid phase separation, the pore sizes are required to be greater than ~7 nm to allow sufficient mass transport. For separation of large biomolecules, large pores up to 100 nm may be required for efficient separation [4].

The size of silica particles and the packing quality can significantly affect the performance of the packed columns. Monodisperse silica particles with smaller diameters are employed to achieve high performance separation. However, coming with the use of smaller particles is the considerably increased back pressure [8]. Half of the particle size may double the separation performance (in terms of theoretical plate numbers) but can also quadruple the back pressure at the same time ($\Delta P \propto 1/d^2$) [4]. Sub-2 μm microspheres are currently the state-of-art on the market for porous silica microspheres. To achieve fast separation on silica microspheres of certain size, a straightforward approach is to increase the flow rate and therefore the pressure drop across the column. Ultrahigh pressure liquid chromatography is thus developed and used. This technique places much stricter requirement on the pumping system and the whole flow system due to the very high operation pressure.

In recent years, core–shell silica particles (solid core and porous shell or superficially porous) have been increasingly used for highly efficient separation with fast flow rate and relatively low back pressure [9]. The solid core plus the porous shell gives a larger particle and thus low operating back pressure while the porous shell and small solid core can provide higher surface area for the separation to occur. For example, the 2.7 μm fused-core silica particles (1.7 μm core and 0.5 μm thick porous shell) could yield efficiency close to the sub-2 μm particles but with operation pressure close to 3 μm particles [10]. The advantage with the core–shell particles as packing materials is that the smaller pore volume reduces the volume present for broadening from longitudinal diffusion (B term in the van Deemter equation). The short diffusion path length can reduce the contribution of the C term due to the fast mass transfer [8,11]. Particle characteristics such as particle size and porous shell thickness can significantly influence separation parameters [12]. As the thickness of the porous shell decreases, the faster mass transfer can lead to improved column efficiency and fast elution time [13,14]. For chromatographic applications, the core–shell silica particles are also widely known as *fused-core*, *solid core* or *superficially porous* particles. There are a number of core–shell particles commercially available, the main ones being Poroshell (Agilent), Halo (Advanced Materials Technology), Cortecs (Waters), Kinetex (Phenomenex) and Accucore (Thermo Fisher Scientific). The columns packed with core–shell particles have been employed in a wide range of applications for analysis and quality control. In this review, we will firstly discuss the types and the general preparation methods for core–shell particles, focusing on the particles used in chromatography. We will then discuss the fundamentals of core–shell particles in HPLC and how it is compared with totally porous particles and monoliths in terms of fast separation with relatively low back pressure. The use of core–shell particles in different chromatography techniques is then described, followed by examples of the applications in different areas. The review is completed with conclusion and outlook for future development in this area.

2. Preparation methods for core–shell particles

By its name, core–shell particles are a class of particles which contain a core and a shell. The core and the shell can be different materials or the same materials with different structures. Fig. 1 shows the schematic representation of different types of core/shell particles. The core and the shell are expressed in different colors. The core may be a single sphere (Fig. 1A) or aggregation of several small spheres (Fig. 1B). It is possible to have a hollow shell with a small sphere inside, a rattle-like or yolk-shell structure (Fig. 1C) [15]. The shell structure can be a continuous layer (Fig. 1A–C) or

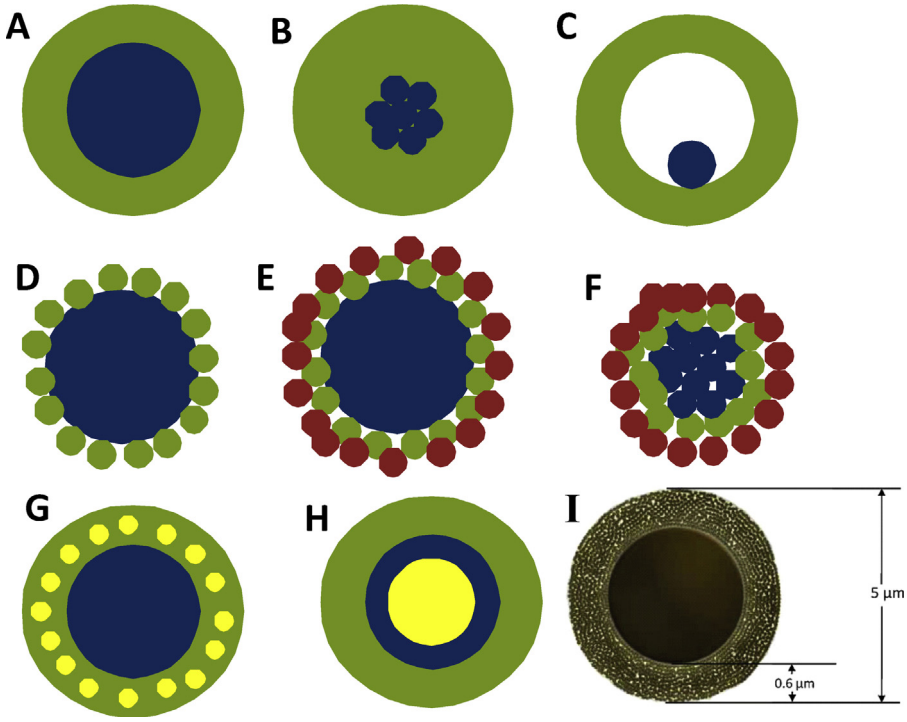

Fig. 1. Schematic representation of different types of core–shell particles.
Image (I) is adapted from Ref. [12] with permission.

attachment of smaller spheres onto a big core sphere (Fig. 1D and E) or aggregated core spheres (Fig. 1F) [16]. Complex core–shell structures may also be made via incorporation of smaller spheres into the shell (Fig. 1G) [17] or with multiple shells (Fig. 1H) [18–20]. Both the core and the shell can be nonporous solid or have desirable porous structures. The core–shell particles used in chromatography are usually made of the same material, silica, but with a solid core and a porous shell (Fig. 1I). The size of the core particle, the shell thickness and the porosity in the shell are tuned to suit different types of chromatographic applications.

Core–shell particles are usually synthesized by a two-step or multiple-step process. The core particles are synthesized first and the shell is then formed on the core particle via different methods, depending on the type of core and shell materials and their morphologies [21]. Core–shell nanoparticles have been mostly investigated, compared to core–shell microspheres. The drive in the preparation of core–shell particles is to combine the desired properties of different materials and structures in order to offer synergistic effect, to stabilize the active particles, or to provide biocompatible properties. For example, Pt_3Co intermetallic cores with a 2–3 atomic-layer-thick Pt shell nanoparticles could enhance their activity and stability as oxygen reduction electrocatalysts [22]. Nanoparticles are coated with a layer of silica to improve the stability in the water medium and biocompatibility for biomedical applications [23,24].

For the core–shell microspheres, many of the examples have been the use of polymer microspheres such as polystyrene (PS) and poly(methyl methacrylate) (PMMA) and silica microspheres as core spheres. The shells are commonly comprised of metal nanoparticles or oxide nanoparticles. A coating of silica layer is often formed on the polymer microspheres. After heat treatment or dissolution to remove the core, hollow spheres can be produced [25]. A rattle-like core–shell structure may be prepared this way when small spheres are present in the core spheres, provided that the small spheres cannot be removed/decomposed when the core spheres are removed [26]. The advantage of core–shell microspheres, compared to the nanospheres, is that they can be easily recovered by simple filtration or centrifugation.

The core–shell microspheres have been used for chromatography as packing materials because the use of nanospheres would cause extremely high operating pressure. Different preparation methods are employed to prepare core–shell microspheres. The mostly used core spheres are monodispersed silica microspheres prepared by the Stöber method [27]. In this section, we describe the methods which have been used to produce core–shell microspheres, particularly for use in liquid chromatography.

2.1. Early attempts

The concept of pellicular particles (a type of core–shell particles often with glass beads or polymer particles as the cores) was initially suggested about 50 years ago [28]. Early generation of pellicular particles and Zipax particles were covered in the review by Guiochon et al. [9]. Kirkland et al. reported the preparation of superficially porous particles ("Poroshell" particles) which were composed of an ultra-pure solid silica core with a thin porous shell. A co-spraying method was initially used, but with the disadvantage of forming some totally porous microspheres that could not be effectively separated from the rest Poroshell particles [29]. A coacervate approach was then employed to improve the quality of Poroshell particles, where the dense silica cores were coated with a urea-formaldehyde/silica sol coacervate film. The resulting particles were sintered to increase particle strength and eliminate unwanted micropores [30]. Rapid separations of polypeptides, proteins, and DNA fragments were performed under gradient conditions with this Poroshell column.

A dry blending method was used to fix small particles onto large particles when the ratio of the diameter of the large particle to that of the small particle is larger than 10:1. The binary mixture particles were mixed in a high-speed air stream caused by the rotation of the rotor and hit repeatedly by the striking pins on the rotor in a hybridizer. The small particles were fixed

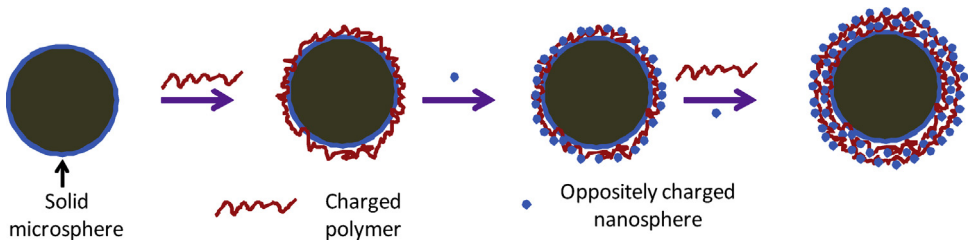

Fig. 2. The schematic representation of forming core–shell silica particles by the LbL approach. The preparation starts with a surface charged solid microsphere. The charged polymer and oppositely charged nanospheres are in turn deposited onto the microsphere surface to produce the core shell particles. Different deposition cycles may be applied to form the shell with different thickness.

to the surface of the larger particles as a result of mechanical actions [31]. For example, core–shell composite microspheres of nonporous silica nanospheres on polyethylene beads were prepared by this approach [31,32]. The diameters of the polyethylene beads were 5, 10, and 20 μm, respectively. Separation of 3 proteins within 10 min was demonstrated by the column packed with such core–shell microspheres [31]. Similarly, a double-coating layer of silica and titania nanospheres on polyethylene beads was generated. When employed as a complex stationary phase for HPLC, the surface double layer caused a change in the surface acidity of the oxides, rather than just a mixture of two stationary phases. The separation of acidic and basic drugs was performed via a multiple retention mechanism [33].

2.2. Layer-by-layer approach via electrostatic interaction

A large percentage of core–shell silica particles for chromatography are now prepared by a layer-by-layer (LbL) approach, particularly for the core–shell particles available on the market [9]. This approach utilizes the electrostatic interaction (and also hydrogen bonding, covalent bonding, van der Waals interactions, etc.) between the positively charged (cationic) and negatively charged (anionic) species to assemble multiple layers together. This technique has been widely used to prepare composites and microcapsules for biomedical applications [34]. Microparticles with suitable surface charges are used as the core and alternative layers (of oppositely charged species, for example, negatively surface-charged silica nanospheres and cationic polymer poly(diallydimethylammonium chloride)) are built up onto the core particles. The removal of the core particles can produce hollow capsules. It is obvious that the core particles should be prepared first and used. The LbL approach via electrostatic interaction has been employed to produce core–shell silica particles, as illustrated in Fig. 2. The core silica particles are firstly bound with a polyelectrolyte (e.g., negatively charged silica particles bound with a cationic polymer). Excess polyelectrolyte is removed by rinsing. The coated core particles are then immersed in a dispersion of nanoparticles with charges opposite from those of the organic polyelectrolyte. This process is repeated by alternating immersions between the polyelectrolyte solution and the nanoparticle suspension until the desired shell thickness achieved [35]. The resulting particles can then be treated thermally to remove the organic polyelectrolyte and produce solid-core porous-shell particles. Fig. 3 shows the scanning electronic microscopic (SEM) and transmission electronic microscopic (TEM) images of one type of core–shell particles, Halo 2.7 μm particles [36]. The solid core and the porous shell can be clearly seen. Similar structures may be observed for other types of core–shell particles, varied in particle size, shell thickness, and pore size. These particle characteristics may be used to explain the difference in chromatographic performances of the Halo and the Kinetex columns. Core–shell particles with the sizes of 1.6 μm, 1.7 μm, 2.5 μm, 2.6 μm, 2.7 μm, 3.6 μm and 5 μm are available from different manufacturers. These particles are frequently evaluated as core–shell particle columns for HPLC separation. The recently developed 1.3 μm core–shell particles showed excellent performance (column efficiency H_{min} = 1.95 μm and separation impedance E_{min} = 2000) and also some limitations (upper pressure limit and extra-column band broadening) [37]. These particles consisted of non-porous cores about 0.9 μm and porous shell < 0.2 μm in thickness. The column packed with 1.3 μm particles gave peak capacity values that were 20–40% higher than the reference column packed with 1.7 μm fully porous particles for the same analysis time [38]. 1.1 μm superficially porous particles with a 0.1 μm porous shell were also synthesized. Non-porous silica spheres (diameter 1 μm) were heated at 1000 °C to produce 0.9 μm particles which were then re-hydroxylated for the LbL coating of different sources of silica nanospheres. The 1.1 μm particles had a surface area of 52 m^2/g and pore diameter of 7.1 nm [13].

More complicatedly, chiral core–shell silica microspheres with trans-(1R,2R)-diaminocyclohexane moiety bridged in the mesoporous shell were synthesized. The chiral nanospheres were firstly formed and then attached onto the non-porous silica core by the LbL method. Rapid enantioseparations (3–12 min) of binaphthol, bromosubstituted binaphthol and biphenathrol were performed by HPLC [39].

Core–shell particles with different ranges of pore sizes in the shell are available to suit different analytes. Particles with shell pore sizes in the range of 8–10 nm are adequate for separating small molecules [12]. Larger molecules require larger pores for efficient separation, e.g., particles with pores 16 nm used for separating peptides and small proteins (Mw of <15 kDa) [40]. Larger superficially porous particles with a pore size of 40 nm allow large molecules (<500 kDa) unrestricted access to the bonded phase and are optimized for protein separations [41].

The productivity of manufacturing core–shell silica particles is low. This is due to the numerous centrifugation steps that are needed to remove extra and loosely bound species in each coating cycle to avoid particle aggregation. A multilayer (ML, film of more than one layer)-by-multilayer (ML) approach was developed to speed the process [42,43]. The silica shells created by the ML-b-ML method had a higher level of porosity than those obtained by the traditional LBL process. The multilayer adsorption phenomenon was attributed to the formation of nanoparticle aggregates, reduced repulsive force between nanoparticles and increased non-electrostatic attraction between nanoparticles and polyelectrolytes [43].

Core–shell silica particles may be further coated with a layer of carbon because carbon is chemically inert and highly stable for a range of test mixtures. 2.7 μm core–shell silica particles were coated with carbon by firstly treated with Al (III). Chemical vapour deposition of carbon onto the silica particles was then conducted at 700 °C for 6 h using hexane as a carbon source. These carbon clad particles gave high efficiency and good peak shapes for fast LC×LC analysis [44]. Coating of core–shell silica particles (2.6 μm) with a chiral selector cellulose tris(4-chloro-3-methylphenylcarbamate) was performed by sonication in tetrahydrofuran and then

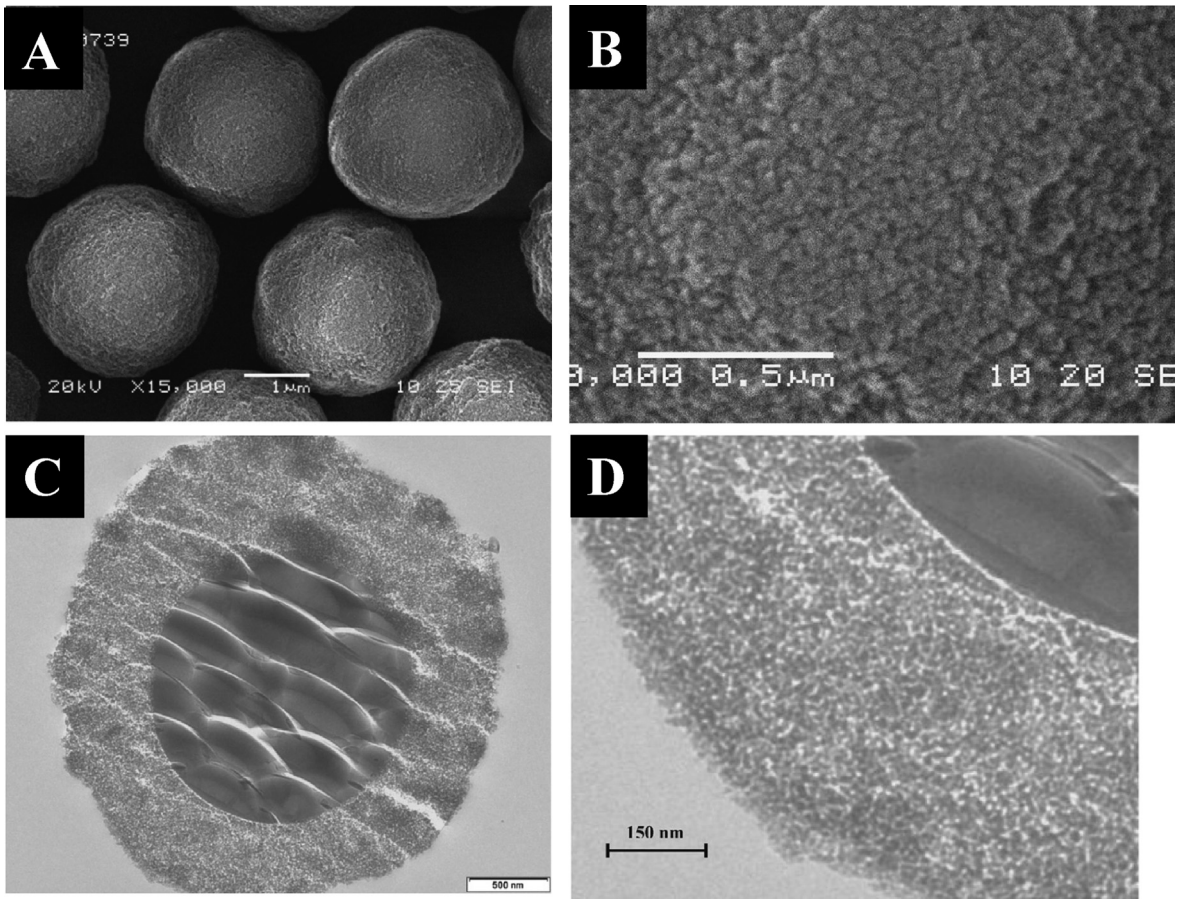

Fig. 3. The morphology and pore structure of Halo 2.7 μm particles. SEM images of (A and B) show the core–shell microsphere and the surface pore structure. TEM image of (C) shows the solid core and porous shell structure while a high resolution TEM image of (D) gives the pore structure in the shell.
Adapted from Ref. [36] with permission.

evaporation at reduced pressure. Better chiral separation was observed particularly at high flow rates, compared to the coated totally porous silica particles [45].

2.3. Shell synthesis on pre-formed cores

Different from the LbL approach, a shell can be formed on a core particle by different synthetic methods. Silica microspheres, polymer microspheres and other particles have been used as the cores to prepare a wide range of core shell particles, for example, silica-polymer core shell particles by silica-supported polymerization [46], core–shell hybrid particles and hollow structures by precipitation polymerization [47], silica–metal–organic frameworks (MOFs) core–shell microspheres [48,49], shaped nanoparticle-shell nanospheres [50]. Hollow shell structures or capsules can be produced when the core polymer particles are removed by thermal treatment or washing [25]. Silica spheres are employed to prepare various inorganic/composite core–shell structures although silica can also be removed by acid etching or alkaline washing to produce hollow structures. Silica is the main source for the core–shell particles used in chromatography. The Stöber method is often used to prepare uniform nonporous silica microspheres and nanospheres, where a base catalyst such as ammonia is used in a system that includes water, alcohol and tetraalkoxysilane [27]. Indeed most of the nonporous core particles in the core–shell particles for HPLC are synthesized by this method. The Stöber method can be modified to produce mesoporous silica microspheres via the introduction of surfactants (cetyltrimethylammonium bromide, CTAB, or non-ionic surfactants Pluronic P123 and F127) into the reactions under suitable conditions as surfactant templates [51,52]. The Stöber approach has also been frequently used to form a silica coating on different shapes and types of colloidal particles [53,54]. In an early example, the sol–gel process of tetraethoxysilane (TEOS) and *n*-octadecyltrimethoxysilane was used to form a coating on silica core spheres in an alkaline solution. The resulting particles were calcined at 550 °C to remove the porogen and produce the solid-core porous-shell particles with a surface area up to 348 m^2/g [55]. Fe_3O_4 nanoparticles were coated with a thin layer of silica, which were further used as the cores to grow another silica layer with perpendicularly aligned mesopores. CTAB was employed as template to generate the mesopores [56]. The monodisperse poly(styrene-co-acrylic acid) spheres were prepared by surfactant-free emulsion polymerization and then used as core particles to form Ag nanoparticles shell by in situ interfacial reduction of $AgNO_3$. A silica layer was further formed on the top via a sol–gel process. These composite core–shell microspheres were used as high performance surface-enhanced Raman spectroscopy substrate and molecular barcode label [57].

Complex core–shell microspheres have been prepared for separation or enrichment of target molecules although not directly for chromatographic applications. Fe_3O_4@SiO_2@layered double hydroxide was synthesized with a SiO_2-coated Fe_3O_4 magnetite core and a layered double hydroxide nanoplatelet shell via an in situ growth method. The composite microspheres showed highly selective adsorption of a histidine-tagged green fluorescent protein [58]. Similarly, magnetic core shell composite microspheres Fe_3O_4@SiO_2-Au@mesoporous SiO_2 were prepared and used as reagentless immunosensor [59]. Fe_3O_4@SiO_2@poly(methyl

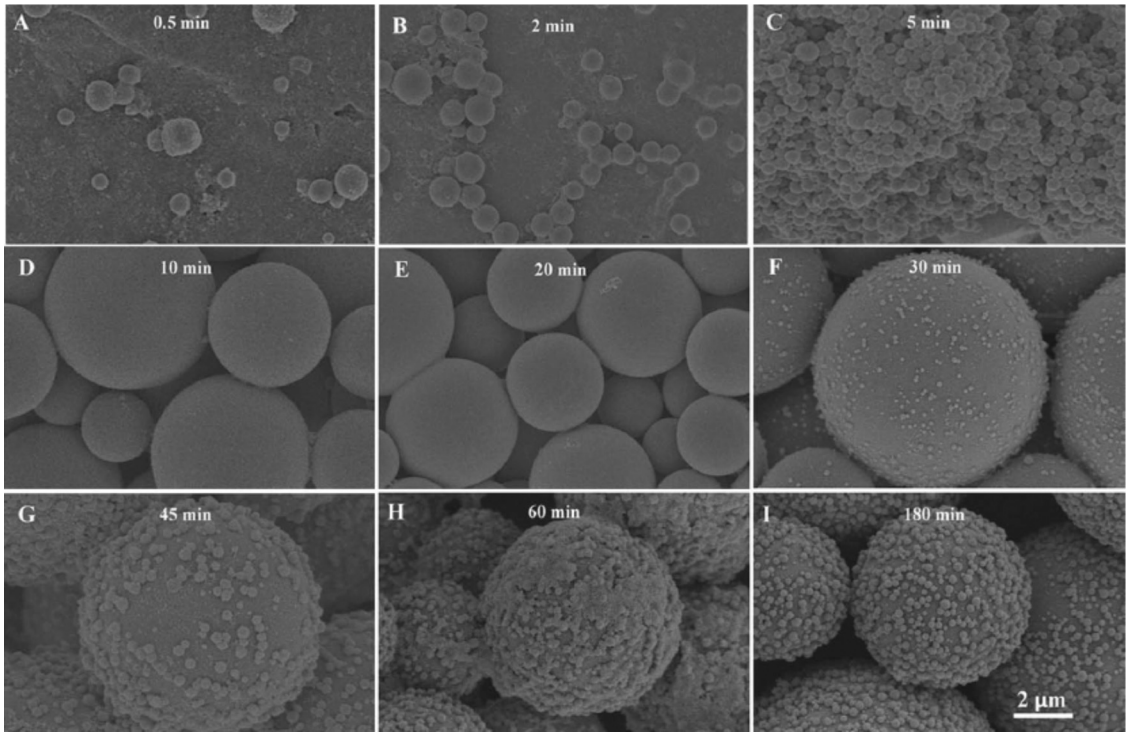

Fig. 4. The SEM images show the structure evolution of silica particles at different reaction times until the SOS particles are formed. Adapted from Ref. [63]. Copyright 2012 Wiley.

methacrylate) core–shell–shell magnetic microspheres were synthesized for efficient enrichment of peptides and proteins for MALDI-ToF MS analysis. The silica-coated spheres were modified with 3-methacryloxypropyltrimethoxysilane to facilitate the next stage surface polymerization [60]. The wider use of magnetic cores is due to the magnetic properties of the resulting particles, which allow facile separation or recovery of the core–shell particles by magnetic force.

2.4. One-pot synthesis and spheres-on-sphere (SOS) silica particles

For the HPLC applications, the core–shell silica particles are usually prepared by the time-consuming LbL approach. A one-pot synthesis of core–shell particles would be highly advantageous, offering potential benefits on reaction time, easier quality control, materials costs, and process simplicity for facile scale-up. It was reported that one-pot synthesis of uniform core–shell nanospheres (around 50 nm) with an Ag nanoparticle core and a thick mesoporous silica shell could be produced by subsequent addition of $AgNO_3$ and TEOS with NaOH as a basic catalyst [61]. One-step synthesis was performed to prepare silica@ resorcinol-formaldehyde (RF) resin nanospheres (around 220 nm) under the Stöber conditions. The reaction utilized the fast reaction rate of forming silica spheres and slow rate of forming RF spheres [62]. However, there have been very limited reports on the one-pot synthesis of core–shell silica microspheres which are suitable for HPLC.

Ahmed et al. reported one-pot synthesis of core–shell silica microspheres with the spheres-on-sphere (SOS) morphology from one single precursor 3-mercaptopropyltrimethoxysilane (MPTMS) [63]. Typically, an aqueous solution of poly(vinyl alcohol) (PVA) and CTAB was firstly prepared. Methanol, ammonia solution, and MPTMS were added to the aqueous solution in turn while stirring. The reaction was stirred for 24 h at room temperature and the SOS silica particles were produced and collected. The SOS particles contained a solid microsphere core (about 5.5 μm) with coated nanospheres of 200 nm. In this one-pot synthesis, however, the SOS particles were formed in two stages (Fig. 4). Silica nanoparticles were formed initially and then grew to microspheres. At the reaction time of 30 min, new silica nanospheres started to form on the microsphere surface. At the reaction time of 180 min, the SOS particles were already formed. The SOS morphology did not change significantly for longer reaction time. The column packed with the SOS particles showed fast separation of protein mixtures at low back pressure. The preparation conditions, such as base catalyst concentration, precursor composition, stirring rate, solvent type, could be varied to tune the microsphere size and the nanosphere size and the density of the nanospheres on the surface of microspheres. Remarkably, a much shorter reaction time (5 min) was sufficient to produce the SOS particles by microwave heating at 40 °C [64].

The SOS particles were further used as support to form additional layer of metal–organic framework (MOF) nanocrystals [49]. MOFs are a type of crystalline porous materials via the linkage of metal ions and organic ligands [65]. Most MOFs exhibit micropores of varied morphologies although great effort (e.g., by ligand extension, combining the synthesis with surfactant templating) has been made to prepare mesoporous MOFs. The pore size, pore shape, and pore surface functionality are well defined in MOFs, which are suitable for highly selective separation of gas molecule or small molecule liquids [65,66]. MOFs have been packed into columns for liquid phase separation [67]. However, low separation efficiency and low column stability are often observed for such columns. This is because MOFs are normally prepared as irregularly shaped microparticles. Packing such particles is very difficult, often leading to low column efficiency, high back pressure and hence crushed particles. To address this problem, MOF nanocrystals could be formed on silica microspheres as a new type of packing material. HKUST-1, a thermally stable cubic MOF with a channel pore size of 1 nm formed by the ligand 1,3,5-benzenetricarboxylic acid and $Cu_2(OAc)_4$ paddlewheel-type secondary building units, was used as a model MOF in the study [49]. HKUST-1 nanocrystals were formed

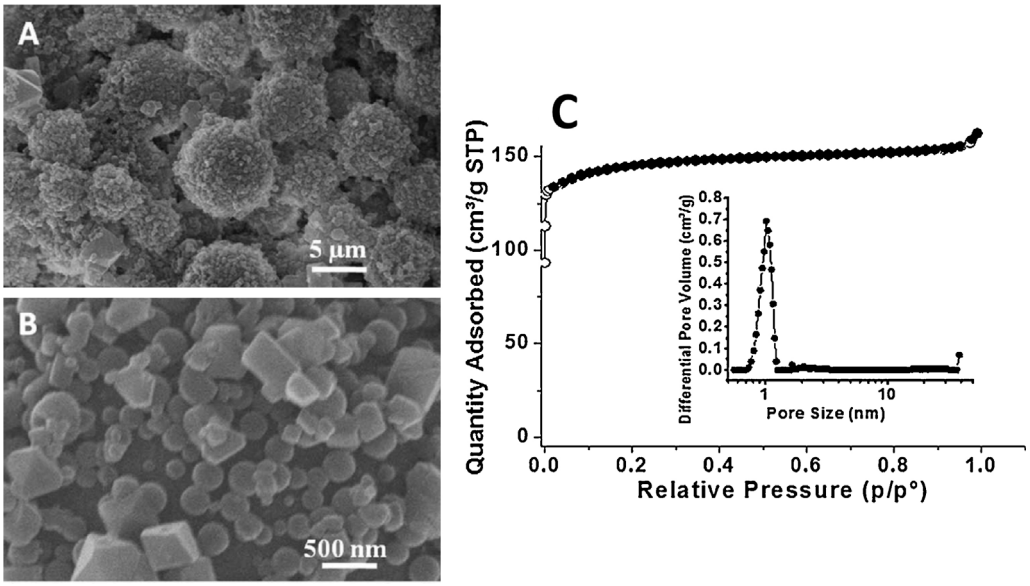

Fig. 5. The core–shell silica-MOF particles. The MOF here is the HKUST-1 nanocrystals. The core–shell particles (A) and the surface morphology of the core–shell particle (B) are shown by SEM imaging at different magnification. The N_2 sorption data (C) shows a microporous material with the pore size distribution around 1 nm.
Adapted from Ref. [49]. Copyright 2013 The Royal Society of Chemistry.

on the SOS microspheres with surface —COOH groups. The silica core was non-porous. The presence of microporous HKUST-1 was confirmed by N_2 sorption analysis (Fig. 5). Compared to the packed HKUST-1 particles, the composite core–shell column showed a fast separation of xylene isomers. Similarly, another type of MOF (ZIF-8) shell consisting of nanocrystals was formed on the commercially available silica microspheres (3 μm) with carboxylic modification. The packed columns showed high column efficiency for the separation of endocrine-disrupting chemicals and pesticides within 7 min [68].

2.5. Droplet-based microfluidic approach

Microfluidics is a highly interdisciplinary research area which involves physics, chemistry, engineering, materials science, and biology. The technology concerns small volumes (from 10^{-9} to 10^{-8} l) of fluids, using channels with dimensions from tens to hundreds of micrometers. It has been widely used to prepare extremely monodisperse emulsions/double emulsions and *microspheres* with complex morphology and compositions [69–71]. Since monodispersed microspheres are known to significantly improve chromatographic performance, the microfluidic method can be very important in developing novel and high performance packing materials for chromatography.

Conventional emulsification methods (e.g., by stirring, homogenization, sonication) produce polydisperse emulsion droplets that can be transformed into spherical microparticles through chemical or physical consolidation. The monodisperse emulsions produced by microfluidics can be used to yield highly uniform microspheres. Functionalized microspheres with complex morphologies including core–shell structures have been realized through shaping, compartmentalizing, and microstructuring [72].

Pickering emulsions (where the droplets are stabilized by small particles) are widely used to produce core–shell particles or capsules. An "inside-out" microfluidic approach was developed to produce monodisperse particle-stabilized emulsions and nanoparticles-decorated microspheres. The nanoparticles are inducted in the droplet phase thus minimizing the waste of nanoparticles [73]. However, a double emulsion approach is probably more used in producing core–shell particles via the microfluidic approach. After forming a double emulsion, the double emulsion droplets can be crosslinked/condensed to form dry core–shell particles. For example, poly(lactide-co-glycolide) (PLG)-dichloromethane solution was injected through an inner capillary into a flow of aqueous alginate solution. The resulting oil-in-water emulsion droplets were then dispersed in a flow of toluene. The crosslinking of alginate and removal of solvent dichloromethane produced PLG-alginate core–shell particles [74]. A single emulsion method could also be used to prepare core–shell particle. As shown in Fig. 6, a silica sol prepared from TEOS was injected into an oil continuous phase containing tetrabutyl titanate (TBT). As soon as the droplet was formed, due to water diffusion, the hydrolysis of TBT occurred at the interface to form a thin gel around the droplet. The full hydrolysis was completed in a solidification bath containing the continuous fluid. This method produced the silica-titania core–shell particles [75]. A simple T-junction microfluidic device was used to produce hierarchical raspberry-like

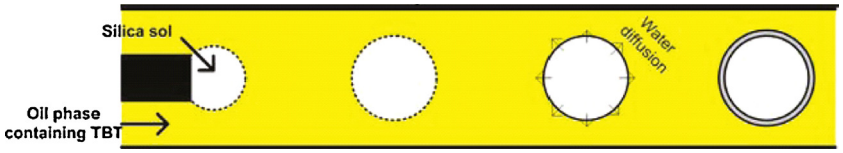

Fig. 6. The scheme represents the preparation of silica-titania core–shell particles by the microfluidics approach. The oil phase is tetrabutyl titanate (TBT) in liquid paraffin with Span 80 (surfactant) and oleic acid.
Adapted from Ref. [75]. Copyright 2011 American Chemical Society.

silica particles [76]. The silica sol formed from TEOS in ethanol and HCl solution was pumped via the inner flow focusing inlet while $NaHCO_3$ solution was pumped through the outer inlet. Hexadecane with a surfactant was used as the continuous phase. The raspberry-like morphology was produced due to the reaction between HCl and $NaHCO_3$ and the formation and escape of CO_2 bubble.

3. The fundamentals of core–shell particles for HPLC

The underlying reasons for the advantages in performance benefits associated with solid-core porous-shell materials has been the subject of much debate and also a high degree of marketing from various manufacturers. Initially the advantages were associated with the better particle size distribution and also the reduction in the resistance to mass transfer terms [2,7]. These initial claims were not quite accurate. There is an improvement on the performance of these types of columns due to these physical parameters, but the observed beneficiary effect due to better particle size distribution and reduced resistance to mass transfer is not as significant as for other contributing factors. In order to better understand how the morphology of solid core particles improves the chromatographic performance, it is necessary to investigate the individual terms of the van Deemter equation [11], written below in modern terminology to determine the effect of the dispersion of the solute molecules within a packed bed environment.

$$h = \frac{B}{v} + A + Cv \tag{1}$$

where h is the reduced plate height, v the reduced velocity, A, B, and C numerical coefficients related to the parameters of the column. Monolithic columns can also offer fast HPLC separation with low back pressure, particularly for large biomolecules. It is important therefore, to also consider the fundamentals of core–shell particles in comparison with monolithic columns.

3.1. A term

The eddy dispersion term of the van Deemter equation has been the interest of many researchers and the mechanistic interpretation of this parameter has improved substantially, although there is still a degree of retrospective fitting of experimental data to allow for optimization of the postulated theory. Specifically the use of the Knox equation [77] which relates an inverse cubic dependency of the linear velocity to the band broadening has proved very successful in modeling of experimentally derived data. The dispersion associated with this term can be rationalized as coming from both the size of the particles and also the quality of the packing. It has been shown that the packing density within a column varies radially as a result of the wall effect, which results in increased band broadening. Thus there are two very distinct components to the 'A' term, one which relates to the short range packing effects associated with a regular packing structure of spheres, and the other one being a longer range effect which occurs due to radial inhomogeneity across the column.

In the initial marketing literature that was associated with the launch of a range of solid core materials, it was suggested that some of the benefits arose because of the tighter particle size distribution which resulted in better packing of the particles. This is an easy concept to visualize, however in practice the variation of the particle size distribution that is quoted for fully porous materials and for solid core materials is simply not large enough to cause an adverse effect, and thus the concept is simply not applicable to the observed high efficiencies associated with solid core materials. A typical solid core particle will be quoted as having a $d_{90/10}$ of 1.1 compared to a fully porous material which has a $d_{90/10}$ of 1.7. It has been shown that this is not a significant enough change to allow for deterioration in the column performance [78]. Indeed the data presented by Gritti et al. [78] suggested that the performance of any form of sub 3 μm particles could be improved by the addition of small volume fraction of larger particles in the range 3–5 μm. In this study, 3 μm and 5 μm particles were mixed to give a bi-modal distribution that probably behaved differently compared to a mono-modal distribution of different variances.

However, it is very evident from a wealth of experimental data that solid core materials do provide a benefit in terms of the 'A' term. Since this parameter is dependent primarily on the particle size and the packing efficiency, the logical conclusion is that the packing is better with solid core materials than with fully porous materials. Solid core materials intrinsically have a rougher surface than fully porous media. As a consequence, there is considerably more shear stress applied to the particles when they are packed. Once the column is packed, it then undergoes a period of consolidation where the pressure is slowly released and the frits and other end fittings are attached. Although it is harder to pack the material, once the material is packed the amount of shear stress required to overcome the frictional forces associated with the roughened surfaces is so great that bed expansion is virtually eliminated, whereas the situation with fully porous materials is very different. Fully porous materials have a much smoother topography resulting in particles that are easier to pack than compared to solid core materials. However, on consolidation of the bed, the lack of a roughened surface means that these particles slide over each other with relative ease compared to the solid core materials, which results in the creation of bed heterogeneity.

3.2. B term

One of the biggest advantages to the use of solid core materials is the reduction in the dead volume of the column. A fully porous material packed into a column will only occupy about one-third of the column volume whereas the amount of space occupied by the solid core material is dramatically increased by about 20–30% [79]. This reduction in the accessible volume of the column results in less longitudinal diffusion occurring within the column. To effectively model the diffusion, it is necessary to consider the various zones within the column media that exist, since diffusion within these zones will be different. On a macroscopic level, there is an effective diffusion coefficient that can be measured. It will be an average of the diffusion occurring within the bulk media and the diffusion occurring within the porous media. Development of a suitable model will allow for the effective diffusion rate to be calculated and will also allow for the effect that the porous layer has on the effective diffusion, and consequently the B term to be determined. There are a variety of models [80–82] that exist that explain dispersion within a multiple zoned bed. However, the most effective one applied to this physical process has been shown to be a model developed by Torquato et al. [81,82] following on from the work of Garnett et al. [80].

Using the same formulas derived by Gritti et al. [83], based on the Garnett–Torquato model:

$$B = \frac{2[1 + 2(1 + \varepsilon_e)\beta - 2\varepsilon_e\xi_2\beta^2]}{\varepsilon_e[1 - (1 - \varepsilon_e)\beta - 2\varepsilon_e\xi_2\beta^2]} \tag{2}$$

where

$$\beta = \frac{(1 - \rho^3)/(1 + \rho^3/2)\Omega - 1}{(1 - \rho^3)/(1 + \rho^3/2)\Omega + 2} \tag{3}$$

and ρ is the ratio of the solid core to the whole diameter of the particle (1 is a solid particle, 0 is a fully porous particle), ξ_2 a three-point parameter for random dispersion of spherical inclusion, ε_e the external column porosity and assumed as 0.4, Ω the ratio of

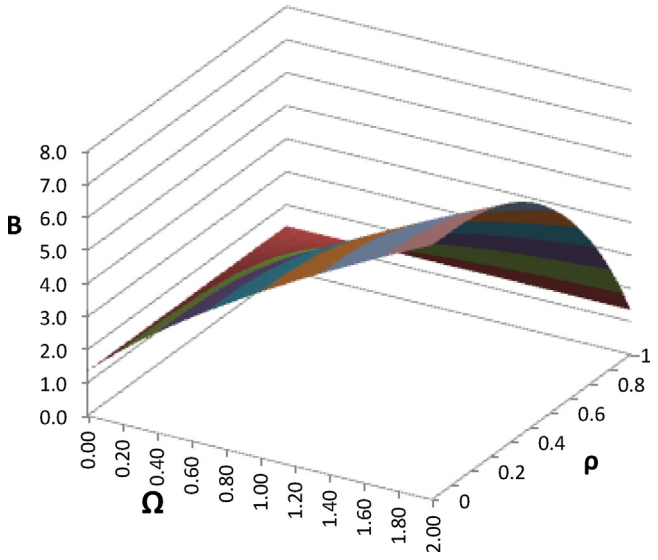

Fig. 7. The minimal value for longitudinal diffusion, the B term, is obtained when either there is limited retention or when the particle does not have any porosity.

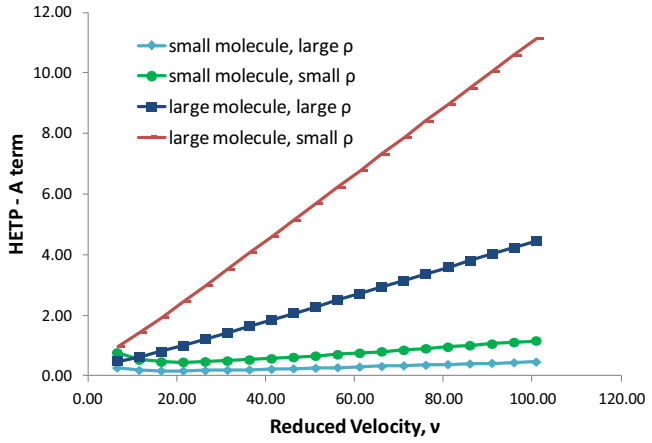

Fig. 8. The plot shows the relationship of B + C terms of the van Deemter equation with reduced velocity. For large molecules where there is reduced diffusion, the C term has a significant effect as the solid core diameter is reduced. Large ρ – 0.9, Small ρ – 0.1, D_m – 1.63e^{-3} (small molecule), D_m – 1.63e^{-5} (large molecule), Ω (small molecule) – 1, Ω (large molecule) – 0.1, d_p – 2.7 μm, k – 3, γ_e – 0.62, ε_e – 0.37, R_c – 4.6.

the effective diffusivity in the porous layer of the particle compared to that in the bulk, effectively giving an indication of the retention of a compound, with higher values being more applicable to more retentive compounds.

A plot can be made which shows the variation of the B term with respect to the retention of the analyte and also the internal porosity of the particle, which can be varied by altering the depth of the porous shell.

The minimal value for longitudinal diffusion, the B term, is obtained when there is limited retention or when the particle does not have any porosity. The diagram in Fig. 7 clearly demonstrates the advantages that reducing the volume of the column by increasing the solid core diameter (increasing ρ) has on the longitudinal diffusion within the column. It can be seen that there is a reduction by 500% as B decreases from 7.7, when Ω is 2, and ρ is 0, to 1.4 when Ω is 0, and ρ is 1. Although this is an extreme example, there is still an appreciable change in the longitudinal diffusion when taking a more realistic value for Ω of 0.14 [79]. It should be mentioned that the improvement in B term is important only in the low flow rage ranges. Generally around and beyond the optimal linear velocity, its impact is almost negligible.

3.3. C term

The final term to consider is the C term or resistance to mass transfer. As with the other terms of the van Deemter model, this has been reviewed and modified since the original publication [11,84]. Modifications to the original publication include the inclusion of mass transfer effect due to different flow velocities within the mobile phase and not just within the stagnant regions of the pore structure.

Initial literature about the launch of the solid core material associated much of the benefits of the technology with the reduced mass transfer effects. However, it was shown by Gritti that for small molecules this is not the case [85]. The major contribution to the reduction in band broadening is associated with the reduction in the B and A dispersion processes. Gritti proposed the following modified equation to determine the contribution of the C term for the band broadening process [85].

$$h_{Long} = \frac{B}{\upsilon} = \frac{2(\gamma_e + (1-\varepsilon_e)/\varepsilon_e(1-\rho^3)/(1+\rho^3/2))}{\upsilon}$$

$$h_{Liquid-Solid} = C\upsilon = \frac{1}{15}\frac{1-\rho^3}{1+(\rho^3/2)}\left(\frac{k_1}{1+k_1}\right)^2 \times \left[\frac{1+2\rho+3\rho^2-\rho^3-5\rho^4}{(1+\rho+\rho^2)^2}\right]\frac{1}{B-2\gamma_e}\upsilon \quad (4)$$

Using this model it is possible to simulate the large and small molecules and to determine the effect that altering the solid core ratio to porous layer will have on the overall chromatographic efficiency. Fig. 8 clearly demonstrates that the porous layer has little effect on the overall H value for small molecules whereas for larger molecules there is a more increased effect.

The contribution of the B term is inversely proportional to the linear velocity and so does not contribute significantly to the overall band broadening at higher linear velocities, which is a focus of Fig. 8. It can be seen from Fig. 8 that although there is a difference in terms of the C term for the small molecule when there are different porous shell thicknesses employed (in this case two extremes were chosen of $\rho = 0.1$ and $\rho = 0.9$). However, the actual value of this number is quite small and as a consequence will have minimal effect on the overall dispersion. Of greater interest though is the data shown in Fig. 8 which highlights the difference between the dispersion observed due to mass transfer effects for larger molecules where the diffusion coefficient is much lower. It is evident that the difference in the C terms in this scenario is contributing significantly to a difference in the overall dispersion seen with a very thin porous layer compared to a virtually fully porous material. Thus it can be concluded that for large molecules such as proteins, or oligonucleotides, a very thin porous layer should be employed to reduce dispersion effects.

So far the dispersion associated with the use of monolithic columns has not been discussed, primarily because the dispersion models that are applicable to the treatment of packed bed columns are not directly transferable to monolithic structures. Silica monolithic columns consist of a continuous, porous rod that has a bimodal porosity [86]. These columns are made of a network of through pores separated by a thin, porous silica or polymeric skeleton. The larger size pores, estimated to be 1.7 μm, measured using mercury intrusion porosimetry [87], allow for movement of the mobile phase, whereas the smaller size pores, measured by nitrogen adsorption was 14 nm [88], generate a large surface area that allows for a sufficient retention of the analytes. The larger

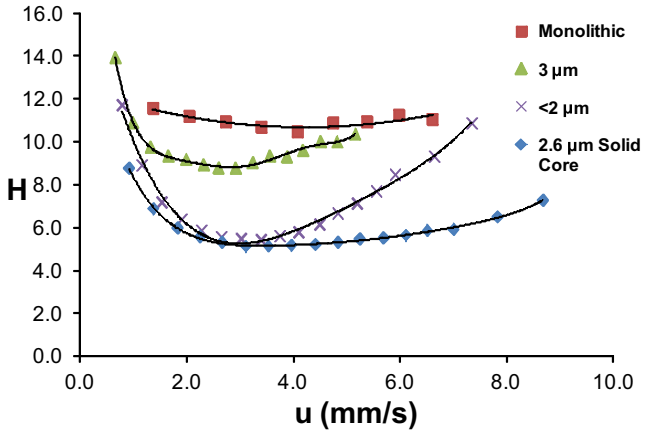

Fig. 9. Efficiency comparison using the van Deemter plots for Accucore 2.6 μm core–shell microspheres, monolithic column, and fully porous 3 μm and sub-2 μm microspheres. All the data were experimentally obtained.

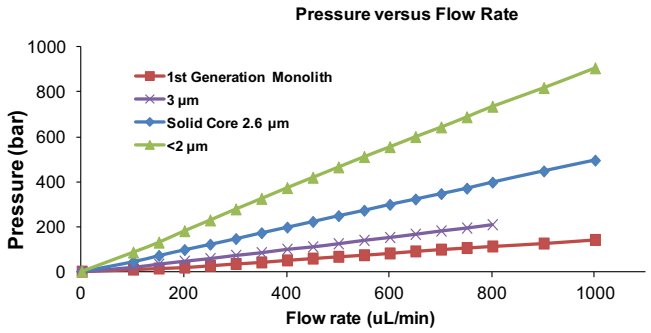

Fig. 10. Comparison of column pressure for Accucore 2.6 μm core–shell microspheres and fully porous 5 and 3 and sub-2 μm microspheres (100 mm × 2.1 mm columns, mobile phase: water/acetonitrile (1:1), temperature 30 °C).
Adapted from Ref. [85]. Copyright© 2012 Chromatography Today.

interconnected pores in the monolithic columns accounts for their advantages over traditional packed columns [86–89], since there is substantially less pressure required to obtain the optimal chromatographic efficiency. Due to the reduced pore depths associated with monolithic structures, there is also a reduction in the resistance to mass transfer term, which allows for use at elevated flow rates without the loss of performance. However, the first generation monoliths suffer from a lack of radial homogeneity, caused by a few factors, including:

- The synthesis of a monolithic column involves an exothermic condensation reaction, with the heat generated being evacuated radially through the monolith, generating a temperature gradient. Because the polycondensation reaction is temperature dependent, it will proceed faster in the column center than at the walls, which might affect the distribution of the local external porosity.
- As part of the manufacturing, the monolithic rod has to be encapsulated by a heat-shrinking PEEK tube around the rod [90,91]. The encapsulation compresses the bed radially and may also cause radial stress and strain.
- It is also feasible that during the polymerization process the monolith is initially attached to the column wall. However, some elastic deformation may occur as the monolith shrinks and breaks away from the column wall.

The radial heterogeneity does affect radial distribution of analytes and also affects the chromatographic efficiency of a column. Indeed, some authors have demonstrated that the column efficiency can be improved by up to 100% by removing this effect [88,92]. The second generation commercial monoliths have a tighter radial pore distribution [93,94], but at the expense of column head pressure. Other approaches can be employed to alleviate the radial heterogeneity [95–98]. This suggests a way of allowing monolithic columns to compete effectively against packed bed column.

The general rate model shows success in explaining the band broadening process occurring within a monolithic column [29–32]. It is feasible to produce a value for HETP (height equivalent theoretical plate), which does allow for some comparisons with packed bed columns.

Fig. 9 is an overlay of H vs. the linear velocity. It can be seen that the overall performance of the solid core material is better than the other columns under evaluation. The worst performed was the monolithic column, with a plate height of double that obtained for the solid core column. However, it should be stressed that this data does not incorporate the amount of pressure required to drive such a separation. It should also be noted that the van Deemter plot for the monolithic column is flatter than the solid core and fully porous materials.

3.4. Kinetic plots

Another area that needs further investigation is the concept that solid core particles give lower back pressure than conventional columns. This is not correct since the resistive forces exhibited by a bed packed with spherical beads are inversely proportional to the square of the particle diameter, in accordance to the Kozeny–Carmen model [99].

$$\frac{\Delta P}{L} = \frac{A\eta(1-\varepsilon_0)^2\mu_0}{\varepsilon_0^3 d_p^2} \tag{5}$$

where A is a constant dependent on the topography of the column, ΔP the pressure drop across column, L the length of column, η the fluid viscosity, ε_0 the porosity of the packed column, μ_0 the superficial velocity, and d_p the particle diameter.

It is not feasible to have a pressure-driven flow through the pores in the porous beads as the diameter of the pores are too small, relative to the interstitial spaces and as a consequence of the lack of a pressure driven flow through the particles, the resistive forces that are present are virtually the same whether the bead is porous or non-porous. Fig. 10 demonstrates this point with the pressure obtained using a 3 μm particle compared to the pressure drop obtained when using a solid core particle have an average diameter of 2.6 μm. The pressure drop observed with a monolithic column and also a sub-2 μm column are also incorporated into the plot [85].

A more discernable measure of the performance of the column does however put the solid core materials in a better light. The use of Poppe or Kinetic plots [100–102] and specifically the use of impedance as devised by Knox and Bristow [103] demonstrate the performance of a column accounting for the flow resistance or the permeability of the column. The mathematics underlying the kinetic plot method is very simple and is based on three 'classical' chromatographic equations.

$$L = NH \tag{6}$$

$$t_0 = \frac{L}{\mu} \tag{7}$$

$$\mu = \frac{\Delta P K_v}{\eta L} \tag{8}$$

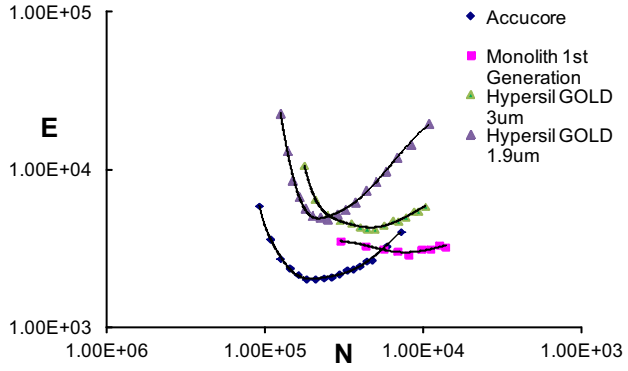

Fig. 11. Performance comparison of Accucore 2.6 μm core–shell microspheres, fully porous 3 and sub-2 μm microspheres, and monolithic columns using kinetic plots.

where L – column length, N – number of plates, H – HETP, μ – linear velocity of mobile phase, t_0 – dead time of the column, ΔP – pressure drop, K_v – column permeability, η – mobile phase viscosity

$$E = \frac{\Delta P t}{\eta N^2} \quad (9)$$

where E is impedance and t is elution time of the test compound.

Kinetic plots are ideally suited to compare the performance of differently shaped or sized liquid chromatography supports, including monolithic supports which are traditionally difficult to compare against spherical particles.

Fig. 11 demonstrates that the fully porous materials have higher impedance, which implies it requires more pressure to get an equivalent separation compared to the monolithic and also the solid core columns. It is interesting to note that with the data presented in Fig. 11, the solid core column would appear to give the best separation per unit measure of pressure where a high efficiency is required, however where a lower efficiency is required then the monolithic column outperforms the other three columns.

The data presented in this section illustrate solid-core chromatographic supports exhibit less band broadening through eddy diffusion and resistance to mass transfer than fully porous chromatographic supports, and also monolithic columns. Models have been presented which demonstrate how the variation of the porous shell can affect the overall chromatographic performance of the column, and in particular the importance of selecting the correct depth of porous layer to optimize the separation for small and large molecules. Models were also presented which have been applied to the physical understanding of the dispersion processes within a monolithic column, and it was stated that one of the limitations of the early designs of monolithic stationary phases was due to the radial heterogeneity of the pore structure caused by the manufacturing process. Direct comparisons of the performance of monolithic columns and packed bed columns can only be achieved if a common scaling factor is used and the introduction of the impedance term allows this to occur [103].

4. Use of core–shell silica microspheres in liquid chromatography

4.1. Reversed-phase HPLC

Reversed-phase analysis is the mostly used mode of HPLC. Comparative studies are performed to investigate the relation between different types of core–shell particles and the column performance. Columns packed with core–shell particles provided high efficiencies with reduced plate height in the range of 1.7–1.5, depending on the test mixtures [104,105]. Destefano et al. reported fast and high resolution separation of naphthalene, virginiamycin, pesticides, and explosives on Halo C18 and C8 columns [104]. The reduced plate height plots for virginiamycin obtained from both columns was significantly lower than 3 μm totally porous particles due to increased mass transfer. Guiochon et al. and others worked with the same type of columns, showing improved separation of large molecules such as proteins, moderate molecular weight peptides, and proteins digests of insulin, lysozyme, myoglobin, and bovine serum albumin [106–109]. Comparing the efficiency of Kinetex C18 with Halo C18, it was reported that Kinetex C18 resulted in better performance with no loss in peak capacity with increasing velocity [110]. It was believed that C term in the HETP plot for the Halo particles was significantly larger, which contradicted with the reduced diffusion distance when using reduced velocities in excess of 10–12. Another study indicated that this increase in performance could be a result of the difference in particles size between the Kinetex (2.6 μm) and Halo (2.7 μm) [109]. The result confirmed the very flat HETP curve, the very low C term of the Kinetex column and its ability to successfully operate at high flow rates while experiencing less efficiency loss than other columns [109]. A systematic evaluation was carried out by Oláh et al. to compare the kinetic performance on Kinetex and Ascentis Express (Sigma–Aldrich) columns by constructing the van Deemter, Knox and Kinetic plots using test mixture of estradiol, levonorgestrel, bicalutamide, and ivermectin [111]. These results indicated that the Kinetex column offered faster mass transfer with a flatter C term. It was suggested that this difference in performance was due to the Ascentis Express column has lower loading capacity and retention factor than even totally porous particles. The relation between the shell pore size and thickness was investigated to establish restricted diffusion of molecules [14,112]. The pore size was found to be the major contributor toward restricted diffusion of large protein molecules at 400 kDa, which was comparable to previous studies on the effect of pore size on molecules diffusion in totally porous particles [112]. The study involved the use of Halo C18 particles with pore sizes of 9, 16 and 40 nm for the separation of proteins such as myosin, ferritin, and β-amylase. Mass transfer kinetic could also be influenced by the shell thickness, thus the separation time almost halved by reducing shell thickness from 350 to 150 nm [14].

4.2. Narrow bore and capillary HPLC

In recent years, column miniaturization has been investigated and tested in order to achieve highly sensitive chromatography. The miniaturized columns are better for handling minute and/or dilute samples, especially in area such as forensic science and sport drug trails. The idea of miniaturization is to provide higher sensitivity and peak capacity than standard columns with minimal dead volume for small sample amounts [113]. Narrow bore columns of 1–2 mm internal diameter (i.d.) can be used on a conventional HPLC system, but the instrument requires modification to reduce dead volume. This becomes more difficult when dealing with capillary columns as the pump needs to be adapted to accommodate low mobile phase flow valves. On-capillary sample injector and detection can be used to reduce dead volume [114]. Systematic studies on the efficiency between narrow bore and analytical type columns showed the same column performance, due to the packing and wall effect [115,116]. Thus different packing methods have been applied such as dry packing [117], high-pressure slurry packing [118], and centripetal force packing [119] to overcome some of the issues. The majority of studies have been done using conventional 3–5 μm silica microspheres. Improved chromatographic performance was obtained by reducing particle size to 1.7 μm, but resulting in an increased backpressure [4]. In this regard, core–shell particles can improve separation efficiencies and speed without having to use very small particles.

Comparative studies have been performed to determine the efficiency of narrow bore core–shell columns (2.1 mm i.d.) with totally porous and monolithic columns [120]. The core–shell particle seemed to give better efficiency and peak asymmetry factors compared to monolithic columns. However, monolithic columns can still offer higher permeability and even lower backpressures at higher linear velocities (up to 8.5 mm/s). This was the case when Kinetex vs. Chromolith columns were tested for isocratic separations of diastereoisomeric flavonoid compounds (silybin and acetylsilybin diastereoisomers). In another study, it was found that the performance of the porous shell particles was significantly negated by the extra-column band broadening especially in narrow bore columns (2.1 mm i.d.) [121]. Gritt et al. carried out systematic studies using different type of core–shell particles and investigated the effect of internal diameter of the column on efficiency [122]. It was shown that depending on the type of silica investigated, the 2.1 and 4.6 i.d. columns gave comparable efficiencies. However, the effect on column efficiency became more dominating with decreasing particle sizes from 4.6 to 1.3 μm (reduced plate height increase slightly from 1.6 to 1.9, respectively) [122].

Currently there are fewer studies published on the application of core–shell particles in capillary columns. Most of those involve capillary electrochromatography. Fanali et al. used 100 μm i.d. capillary packed with 2.6 μm core–shell Kinetex C18 particles for the analysis of different brands of green and black tea constituents [123]. Sharper peaks in the chromatogram and shorter analysis time were observed, compared to sub-2 μm C18 particles. Accurate mass detection of the tea constituents was determined by coupling with the mass spectrometer (MS). Due to the use of capillary column there was no need to split flow prior to the MS interface, hence resulted in better signal and sensitivity. In another study, phenylhexyl core–shell Phenomenex particles were packed into capillary columns with 25, 50, 75, 100 and 150 μm i.d. to be used to separate five aromatic hydrocarbons [124]. Higher plate number per meter was obtained with decreasing capillary diameter without significant decrease of efficiency, with the highest plate number observed for 25 μm capillary. These results indicated that the extra band broadening observed with narrow bore columns were almost excluded in capillary columns.

4.3. HILIC separation

Unbonded silica phase is used to increase retention of polar compounds such as carbohydrates, peptides and nucleic acid components. The separation can be carried out under hydrophilic interaction liquid chromatography (HILIC) condition [125,126]. A Halo Penta-HILIC column demonstrated the ability for fast separation of a mixture of nucleosides and bases with excellent peak shapes and efficiency in less than 9 min [127]. It was also successfully used for the analysis of abuse and metabolites drugs such as cocain, meperidine and methamphetamine. A comparative study with porous sub-2 μm and porous shell 2.7 μm was carried out under HILIC conditions. The fused-core column offered d a faster separation time and a backpressure two times lower, but generated 30% lower efficiency than predicted [128].

The core–shell particles can be also used in supercritical fluid chromatography mode as it offers faster mass transfer and is environmentally friendly. A Kinetex HILIC column showed almost 50% increase in efficiency and halved the time of separation when compared with totally porous particles using gaseous CO_2 as the mobile phase [129].

4.4. Chiral separation

Another area of chromatography is chiral separation, which accounts for analysis of over one-third of marketed drugs. A few chiral phases are commercially available such as polysaccharides [130,131], cylodextrines [132], and others [133]. A recent study reported the coating of Kinetex particles with polysaccharide chiral selectors [45]. Higher selectivity was observed for the separation of enantiomers of trans-stilbene oxide, benzoin and 2,2′-dihydroxyl-6,6′-dimethylbiphenyl. But the performance was relatively similar to totally porous particles. Wu et al. reported the bridging of chiral ligand in the porous shell with a diaminocyclohexane moiety [39]. Rapid chiral separation was demonstrated. The column packed with the chiral core–shell particles exhibited better performance than the column packed with the functionalized periodic mesoporous organosilicas.

4.5. Capillary electrochromatography separation

Capillary electrochromatography (CEC) is a separation technique in which the mobile phase is driven by an electro-osmotic flow rather than pressure in HPLC. CEC combines the separation and selectivity of HPLC and the high efficiency of capillary electrophoresis (CE) [134]. The role of stationary phase has been investigated for improved separation. Variety of stationary phases has been tested such as silica and polymeric materials with different bonding phases [134–136]. Core–shell particles have shown a great success in conventional liquid chromatography. However, the use of these particles in CEC is very limited so far. An interesting study by Fanali et al. compared the performance of capillary columns packed with totally porous and core–shell silica particles for chiral separation in CEC mode [137]. The particles were coated with cellulose tris(4-chloro-3-methylphenylcarbanate), which is a polymer-based chiral selector. The capillary column packed with the core–shell 2.8 μm particles showed baseline separation of warfarin and temazpam with excellent peak shapes compared to 3 μm totally porous particles. This study has shown that porous shell particles can perform in CEC mode without any loss of resolution or efficiency [137]. It would be interesting if these particles can be expanded into separation of other mixtures.

4.6. Two dimensional liquid chromatography

Two dimensional liquid chromatography (2D-LC) is a technique where the injected sample is analyzed by the use of two separation stages. This is accomplished by injecting the eluent from the first column onto a second column. While applications exist which utilize a pair of identical phases, the two phases do not necessarily need to be the same. With an alternate phase in the second column (or the second dimension), it becomes possible to separate analytes that are poorly resolved by the first column or to use the first dimension as a clean-up step. The main advantage of this method over conventional one dimensional chromatography is the potential for a large increase in peak capacity. This can be achieved without requiring particularly efficient separations from either column as, under ideal conditions, it is possible to obtain a total peak capacity equal to the product of the first and second separations [138]. The major disadvantage is the long timescale involved in comprehensive 2D-LC. Run times can exceed several hours, however theoretical peak capacities in the thousands can be achieved if a longer analysis time is acceptable [139,140].

Examples of the use of fused core particles in 2D-LC include pharmaceutical and food analysis. In one study, the increased resolving power when using the reversed phase dual fused-core secondary columns confirmed the presence of minor components from the degradation of a drug compound. Very fast gradient separations were achieved at ambient temperature without excessive backpressure and without compromising optimal 1st dimension sampling rates [141]. In the analysis of pesticides in food, a totally porous HILIC column provided fast on-line clean-up of the

samples in the first dimension, followed by analysis using a C18 core shell column. The method was shown to be capable of analysing over 300 compounds with good sensitivity and robustness [142]. A layer of carbon could be deposited on 2.7 μm superficially porous silica microspheres without causing pore blockage. The use of these carbon clad core–shell silica as a new packing material in fast 2D-LC as the second dimension improved the peak capacity [44].

5. Applications of core–shell particles columns

In the above section, when discussing the types of liquid chromatography employing core–shell particles columns, some applications have been covered. In this section, by giving some more but not exhaustive example applications, we intend to show that the core–shell particles columns can be used for analyzing a large variety of samples in different fields.

5.1. Proteins, peptides and biomacromolecules

Kirkland et al. recently published an overview describing families of fused-core particles and their optimization in separating particular groups of compounds based on their size and properties [127]. The original fused-core particles developed by Advanced Materials Technology aimed at separation of small molecules were 2.7 μm in diameter with a 0.5 μm shell, 9 nm pores and a surface area of 135 m^2/g. Due to the poor diffusion by larger analytes into the pore system, fused-core particles with 16 nm pores were introduced which were more suitable for the separation of peptides and small proteins up to around 15 kDa [143]. A test mixture of small proteins was analyzed on both 9 and 16 nm fused-core silica particles, with the latter providing far superior peak shapes. Most recently, fused-core particles with even wider pores were introduced for the analysis of very large proteins and biomacromolecules [144]. Analytes up to around 400 kDa were efficiently separated using this material without observing any restrictive diffusion that would hinder the chromatographic performance. When compared with fully porous particles, the column packed with fused-core particles provided better chromatographic performance. The van Deemter plot showed that the efficiency was higher for the fused-core column at the minimum plate height and showed a far smaller increase in plate height as the mobile phase velocity was increased – a result of the superior mass transfer allowed by the thin porous shell [12].

Wagner et al. systematically investigated the effects of particle size, pore size, shell thickness and bonded phase effects on the analysis of biomacromolecules [112]. By altering the physical properties of the particles they were able to optimize these parameters to produce particles capable of delivering fast, efficient separation of specific molecular sizes. Two types of particles were used in this study, a 2.7 μm overall diameter with 0.35 μm shell thickness and 3.4 μm particles with a 0.2 μm shell, both of which had a wide pore size of 40 nm. A comparison between the stationary phases with differing pore size in Fig. 12 shows restricted diffusion for larger molecules such as ribonuclease A and insulin on the 9 nm C18 phase, and that increasing the pore size to 16 and 40 nm improves the peak shape and selectivity. Unusual results were obtained when van Deemter plots were produced for the proteins studied, where the larger diameter particle showed a smaller plate height, especially at higher mobile phase velocity which could be attributed to the reduced shell thickness (smaller C term). When compared with 3 μm totally porous particles, the superior mass transfer of the fused-core particles resulted in faster protein separation and improved resolution.

Staub et al. made comparisons between fully porous sub-2 μm and sub-3 μm core–shell particles for the analysis of peptides,

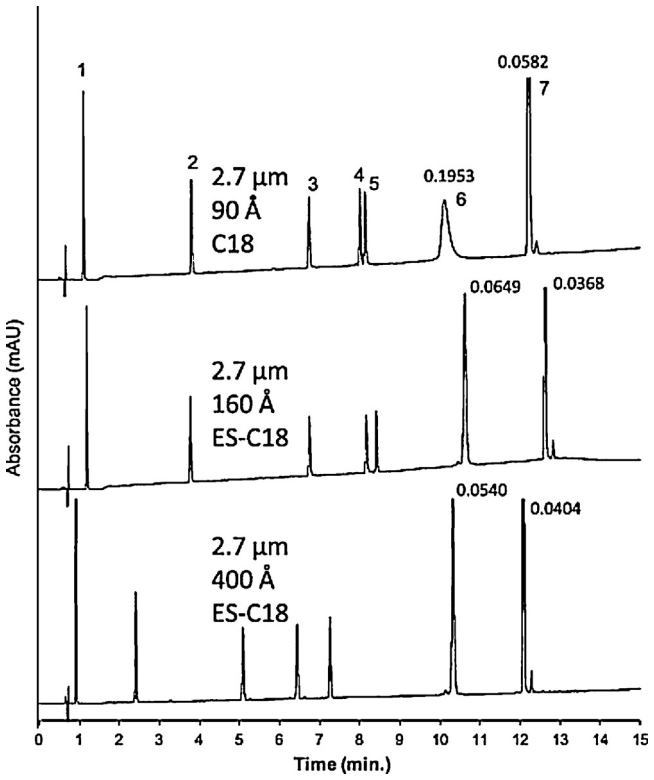

Fig. 12. Effect of pore size. Columns: 100 mm × 4.6 mm; particles: 2.7 μm; mobile phase – A: 10% acetonitrile/90% of 0.1% TFA; B: 70% acetonitrile/30% of 0.1% TFA; gradient: 0–50% B in 15 min; flow rate: 1.5 mL/min; temperature: 30 °C; injection: 5 μL; instrument: Agilent 1100; detection: 220 nm; peak identities: (1) Gly-Tyr – 238 g/mol, (2) Val-Tyr-Val – 380 g/mol, (3) methionine enkephalin – 574 g/mol, (4) angiotensin II – 1046 g/mol, (5) leucine enkephalin – 556 g/mol, (6) ribonuclease A – 13,700 g/mol, (7) insulin – 5800 g/mol; peak widths in minutes measured at 50% height for ribonuclease A and insulin.
Adapted from Ref. [112].

proteins and protein digests [145]. Chromatographic performance was found to be similar between the two types of silica. Analysis of a test mixture containing six peptides using a selection of C18 core–shell and C18 sub-2 μm columns showed comparable results for all in terms of resolution and peak capacity. The overlaid chromatograms are shown in Fig. 13. All columns were able to

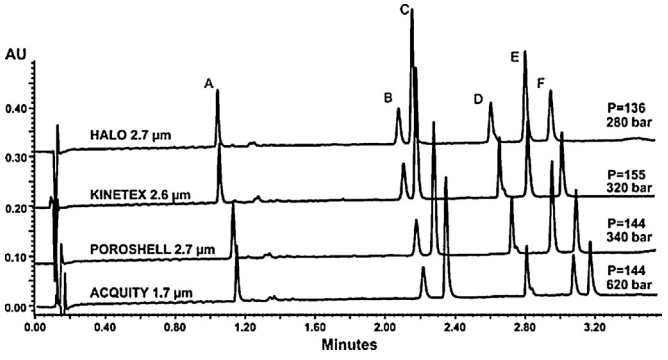

Fig. 13. Chromatograms of (A) Arg-vasopressine (25 μg/mL), (B) peptide 1 (20 μg/mL), (C) peptide 2 (10 μg/mL), (D) insulin (30 μg/mL), (E) peptide 3 (25 μg/mL), (F) peptide 4 (50 μg/mL) separated on three fused-core columns: Halo C18, 50 mm × 2.1 mm, 2.7 μm; Poroshell 120 EC-C18, 50 mm × 2.1 mm, 2.7 μm; Kinetex C18, 50 mm × 2.1 mm, 2.6 μm and one UHPLC column: Acquity C18 BEH 120, 50 mm × 2.1 mm, 1.7 μm. Mobile phase: A: water/0.1% TFA; B: acetonitrile/0.1% TFA; gradient: 5–50% B in 4 min; flow rate: 1000 μL/min; temperature: 50 °C; injection: 2 μL; detection: 214 nm.
Adapted from Ref. [145].

fully separate the mixture within 3.5 min. However, the fused-core columns generated little more than half the backpressure compared with the sub-2 μm column. Each column was also tested using a tryptic digest of four proteins, equivalent to approximately 160 peptides, with a goal of improving peak capacity and resolution. Again, the results were comparable between the four columns and all yielded close to the target number of peaks, demonstrating the potential use in analysing protein digests.

Ruta et al. evaluated the performance of core–shell particles on a range of pharmaceutically relevant compounds [146]. A test mixture of 13 analytes including basic drugs and acidic compounds was investigated using columns packed with a variety of core–shell and sub-2 μm particles. The same elution order was seen on four different columns under acidic conditions as any residual silanols on the surface of the stationary phase were neutral at pH 2.7 and a reversed phase mechanism should govern the retention. There were some changes observed in selectivity between columns, but with some small adjustments it should be possible to transfer a method developed for the sub-2 μm column to a core–shell column. Under neutral conditions, silanols were mostly deprotonated and thus changes in retention and selectivity were observed due to different silanol activity between columns. The peaks found to be tailing under acidic conditions showed improved width and asymmtery at pH 6.85. Selectivity between columns was similar, though there were certain peaks where one type of particle provided superior resolving power than the other, highlighting the potential for method transfer.

Fekete and Guillarme described the use of 1.3 μm core–shell particles for separation of small molecules and peptides [147]. Looking at the kinetic properties of these small particles, the van Deemter plot was extremely flat over the entire range of mobile phase velocity. In isocratic mode, the new core–shell 1.3 μm particles provided excellent efficiency for peptides as the column could be run at the optimal flow rate thus minimizing longitudinal diffusion. When analysing peptides in the gradient elution mode, the 1.3 μm particles offered the fastest separation up to around a peak capacity of 700.

5.2. Food analysis

As the use of fused-core particles is a comparatively recent trend in chromatography, their use in fields such as food analysis is still emerging. Some examples include the determination of toltrazuril and its metabolites [148], corticosteroids [149], chloramphenicol [150], and flavonoids [151] in foodstuffs and the detection of neonicotinoids in beeswax [152]. The latter described a new method to detect a total of 7 neonicotinoids in beeswax using liquid chromatography coupled to electrospray ionization mass spectrometry (ESI-MS) [152]. Initial stock solutions were tested to develop the method before samples taken from 30 apiaries located close to fruit orchards were analyzed. In total 11 samples were found to show neonicotinoid residues at low levels (11–153 μg/kg). In the development, strong ion suppression was observed and it was necessary to construct matrix calibration curves, however the method demonstrated consistent and reliable results and optimization of the preparation method allowed for good recoveries at different concentrations.

Another use of fused-core columns is in the detection of contaminents originating from food packaging, such as the migration of compounds [153]. One application is concerned with detecting bisphenol compounds in soft drinks and canned foods using a liquid chromatography–tandem mass spectrometry method (LC–MS/MS) [154]. Epoxy-based laquers are commonly used as a coating on the inside of food containers to reduce food spoilage and prevent degradation of the container itself. Some coatings are based on polymerization of bisphenol A-diglycicyl ether (BADGE) or bisphenol F-diglycidyl ether (BFDGE) which can release these compounds and derivatives into the packed foods. As well as this, hydrolysed and chlorinated derivatives such as BADGE·H_2O, BADGE·$2H_2O$, BFDGE·H_2O, BFDGE·$2H_2O$, BADGE·HCl, BADGE·2HCl and BADGE·HCl·H_2O can also be produced when the coating is thermally treated or comes into contact with acidic and aqueous contents.

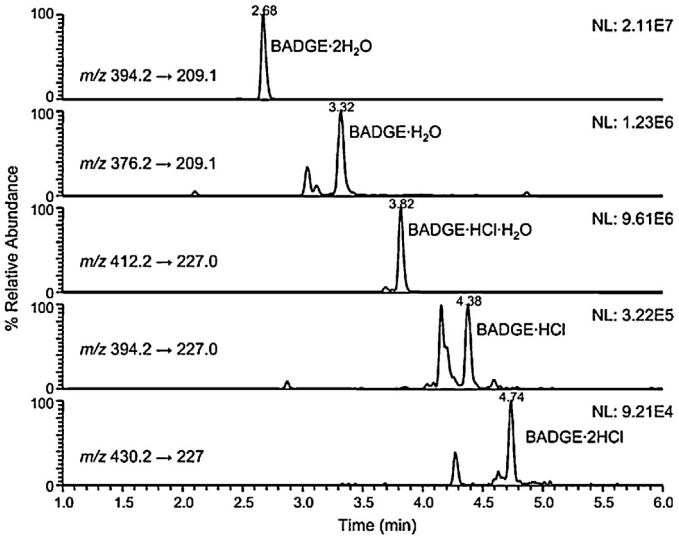

Fig. 14. LC–MS/MS chromatogram in SRM acquisition mode for the analysis of BADGEs in asparagus.
Adapted from Ref. [154].

Current LC–MS/MS methods of analysis use conventional 3–5 μm particles, leading to long analysis times when detecting both BADGE and BFDGEs in the same run. The aim was to develop a faster method using LC–MS/MS. In this study a fused core material was chosen over a sub-2 μm column as the lower back pressure generated enabled a longer column length to be utilized [154]. Efficient separation of BADGEs in asparagus was achieved using the fused-core particles, with a run time of under 5 min. Fig. 14 shows the chromatograms in which BADGE·H_2O, BADGE·$2H_2O$, BADGE·HCl, BADGE·2HCl and BADGE·HCl·H_2O were detected.

Another investigation by the same group was concerned with analysis of bisphenols in canned soft drinks [155]. Bisphenol A (BPA) is widely used in the production of the resin coating of cans and therefore foodstuffs may be expected to contain traces of BPA. As there is an abundance of toxicity data for BPA, limits are in place on migrations limits from coating to food as well as tolerable daily intake. Due to these restrictions, other bisphenol compounds (BPs) are being considered for use in place of BPA, however there is significantly less published data on these alternatives and for most, no limits have yet been proposed.

An online solid phase extraction (SPE) LC–MS/MS method was developed on the same fused core material as in the previous example. The SPE LC–MS/MS method was then used for the analysis of bisphenols in eleven canned soft drinks. BPA was detected in most samples and bisphenol F found in only two. The rest of the BPs were not indentified. The use of a SPE clean up step allowed the analysis of BPs at concentrations lower than 100 ng/L and the method was shown to be robust and sensitive enough for routine analysis of BPs.

5.3. Environmental

Fused-core technology has also found its way into the analysis of water samples, including drinking water, surface water and sewage. Various techniques are used for the detection of antibiotics [156], drugs of abuse [157–159], oestrogens [160], bisphenols

[161], pharmaceuticals [162], herbicides, and pesticides. Pesticides are widely used in agriculture to protect crops from threats such as weeds, disease and insects, however they can also cause environmental pollution in water and wildlife as well as serious health effects on human beings. As such maximum contamination values in drinking water for a number of pesticides have been established by several legislative bodies.

As pesticides are usually detected at low concentrations, highly sensitive techniques are required to analyze them. Off-line SPE followed by gas or liquid chromatography coupled to mass spectrometry (GC–MS or LC–MS) is the most common approach. The downside is that off-line SPE methods are time consuming and typically require high sample volumes. Hurtado-Sánchez et al. developed a fast, sensitive method utilizing on-line SPE coupled with HPLC and tandem mass spectrometry (SPE–LC–MS/MS) [163]. The method was initially optimized and validated by spiking water samples with a known concentration of a number of pesticides to assess the precision and linearity of the method, as well as establish detection limits. Matrix effects were also studied and for most compounds were found to be diminished by dilution of samples with pure water.

Surface water samples were then collected and analyzed for polar pesticides using this method. A column (50 mm × 4.6 mm) packed with Poroshell 120 EC-C18 particles (2.7 μm) was used. Among the samples tested, the highest number of pesticides were detected in irrigation waters from agricultural sources. Six compounds were found at trace levels above the detection limit. In the validation of the method, three compounds that were found not to be retained with off-line SPE were also sucessfully analyzed. Overall the method was shown to be highly effective and suitable for use in routine analysis.

Another study by Zhang et al. presented an alternative SPE and HPLC–MS/MS method to analyze a range of herbicides in environmental water [164]. The method was validated by addition of target herbicides into water samples at two concentrations. The recoveries of 31 compounds were monitored, the majority of which achieved acceptable values of recovery and repeatability. Again, matrix effects were studied which found that the majority of herbicides exhibited ion suppression of ≤20%. The method was then applied to the analysis of stormwater samples. 24 of the 31 monitored herbicides were detected in a wide range of concentrations. Comparison of the fused-core HPLC column (Kinetex C18 100 Å, 50 mm × 2.1 mm, 2.6 μm) to a conventional 5 μm material showed an improvement in efficiency and the run time was halved.

Chocholouš et al. looked at the advantages of fused-core technology in the determination of phenolic acids using a sequential injection chromatography (SIC) method [165]. These compounds are hydroxylated derivatives of benzoic or cinnamic acid and are commonly found in plants. Phenolic acids have attracted considerable interest in the past few years because of their potential health benefits. They are powerful antioxidants which show antibacterial, antiviral, anti-carcinogenic, anti-inflammatory and vasodilatory action.

Typical stationary phases used in SIC are monolithic sorbents with C18 or surfactant functionalization. By contrast, core–shell particles are available with many different chemistries. The use of alternative phases allows for extended selectivity by increasing the number of interactions between the analytes and the stationary phase. Separation conditions were optimized for three core–shell columns with different functionalization and their ability to separate a total of seven phenolic acids was compared.

Using a reversed phase amide column provided the highest chromatographic resolution and allowed for complete baseline separation of protocatechuic, syringic, vanillic, ferulic, sinapinic, p-coumaric and o-coumaric acids. Phenyl-Hexyl and C18 columns were unable to completely separate the tested mixture, with some co-elution observed. The work demonstrated fast chromatographic separation as well as a simple, fast and low-cost analysis.

Vinci et al. developed a liquid chromatography method to determine polycyclic aromatic hydrocarbons (PAHs) in rainwater [166]. Many PAHs are considered as carcinogens, benzo[a]pyrene for example has been described as a human carcinogen since 1987. In general PAHs are not detected individually, but in mixtures. 16 have been monitored by the United States Environmental Protection Agency (EPA) and listed as priority organic pollutants due to their environmental effects.

The method was optimized by testing a standard mixture containing all 16 EPA-PAHs which gave fast separation of all compounds with good resolution and sensitivity. Chromatographic performance can be compared to columns packed with a 1.8 μm totally porous material in terms of elution time and solvent consumption, but with the advantage of far lower operating pressure [167]. When applied to the analysis of rainwater samples, PAHs were detected in each that were analyzed and the method was shown to be viable for trace analysis of environmental water samples.

6. Conclusions and outlook

Core–shell particles can have different structures and morphologies. Core–shell particles particularly nanospheres have been widely investigated in materials science and are exploited for a very wide range of applications. However, for chromatography, core–shell microspheres are utilized. In this review, the types of core–shell particles and the relevant preparation methods are explained. We have focused on the methods that can be used to produce core–shell microspheres for use in chromatography. Core–shell (or fused-core) silica microspheres are mostly used as the packing materials for HPLC columns. The LbL approach is the main method for the preparation of such particles. Monodispersed microspheres are always preferred as packing materials. The microfluidic approach is very effective in producing monodispersed particles and therefore may have potential for use in chromatography. However, the versatility and low productivity of this approach have limited its application for production of HPLC packing materials. To address the time-consuming procedures in the LbL approach, a one-pot synthesis method has been developed to form a type of core–shell particles, namely, SOS silica microspheres, which have shown equivalent or better performance in separation of certain mixtures, compared to the conventional core–shell silica particles. New core–shell particles (e.g., silica-MOF microspheres) have also been developed to improve the separation of difficult mixtures.

With the excellent performance and low back pressure from core–shell particles columns, some argue that this may be down to the extremely monodispersed core–shell particles. This is unlikely to be the single reason. We have discussed, evidenced with test data, how the core–shell particles perform by means of A, B, C terms in the van Deemter equation and kinetic plots. The performance of core–shell particles has been compared to totally porous silica microspheres (especially sub-2 μm) and monolithic columns. For investigation and applications, core–shell particle columns are mostly used in the reversed phase HPLC. Due to their proven performance, core–shell particles have also been employed in HILIC, narrow bore/capillary columns, chiral separations and CEC. The applications of core–shell particles columns are described and explained, demonstrating the increasingly wide use of core–shell particles in HPLC.

There is no doubt that core–shell particles will be continuously evaluated and investigated for highly efficient separation of new and complex mixtures. The challenges lie in the separation of isomers or molecules with very similar structures/properties and

complex samples from biological and life sciences. Chiral separation is also extremely important and challenging. Researchers and manufacturers will need to carefully adjust particle size, shell thickness and pore sizes/porosity, and the surface functionalities in the pores, to address various separation needs. It is also important to improve the packing methods and instrumentation to allow the separations to be performed under optimal conditions. Since the separations occur on the stationary phase or the packing material, the most critical point may be the fabrication of new functional materials in order to significantly improve the separation performance. New methods/procedures will be developed to design and produce novel functional core–shell particles and other types of packing materials. In doing so, materials science and chemical functionalization will play a crucial role.

Acknowledgements

We are grateful for the CASE Award studentship to R.H. by the EPSRC and Thermo Fisher Scientific. We thank Prof. Peter Myers for constructive discussion and reading through this manuscript.

References

[1] L.R. Snyder, J.J. Kirkland, J.W. Dolan, Introduction to Modern Liquid Chromatography, 3rd ed., John Wiley & Sons, 2010.
[2] S. Fekete, E. Oláh, J. Fekete, J. Chromatogr. A 1228 (2012) 57.
[3] G. Guiochon, J. Chromatogr. A 1168 (2007) 101.
[4] K.K. Unger, R. Skudas, M.M. Schulte, J. Chromatogr. A 1184 (2008) 393.
[5] F. Svec, J. Chromatogr. A 1217 (2010) 902.
[6] R. Bandari, W. Knolle, A. Prager-Duschke, H.J. Glaesel, M.R. Buchmeiser, Macromol. Chem. Phys. 208 (2007) 1428.
[7] J.E. Macnair, K.C. Lewis, J.W. Jorgenson, Anal. Chem. 69 (1997) 983.
[8] N. Wu, A.W. Clausen, J. Sep. Sci. 30 (2007) 1167.
[9] G. Guiochona, F. Gritti, J. Chromatogr. A 1218 (2011) 1915.
[10] R.W. Brice, X. Zhang, L.A. Colón, J. Sep. Sci. 32 (2009) 2723.
[11] J.J. van Deemter, F.J. Zuiderweg, A. Kinkenberg, Chem. Eng. Sci. 5 (1956) 271.
[12] J.J. DeStefano, S.A. Schuster, J.M. Lawhorn, J.J. Kirkland, J. Chromatogr. A 1258 (2012) 76.
[13] L.E. Blue, J.W. Jorgenson, J. Chromatogr. A 1218 (2011) 7989.
[14] J.O. Omamogho, J.P. Hanrahan, J. Tobin, J.D. Glennon, J. Chromatogr. A 1218 (2011) 1942.
[15] J. Liu, S.Z. Qiao, J.S. Chen, X.W. Lou, X. Xing, G.Q. Lu, Chem. Commun. 47 (2011) 12578.
[16] X. Zhang, H. Niu, W. Li, Y. Shi, Y. Cai, Chem. Commun. 47 (2011) 4454.
[17] N. Insin, J.B. Tracy, H. Lee, J.P. Zimmer, R.M. Westervelt, M.G. Bawendl, ACS Nano 2 (2008) 197.
[18] X. Lai, J. Li, B.A. Korgel, Z. Dong, Z. Li, F. Su, J. Du, D. Wang, Angew. Chem. Int. Ed. 50 (2011) 2738.
[19] H.H. Park, K. Woo, J.P. Ahn, Sci. Rep. 3 (2013) 1497.
[20] R. Gui, A. Wan, H. Jin, Analyst 138 (2013) 5956.
[21] R.G. Chaudhuri, S. Paria, Chem. Rev. 112 (2012) 2373.
[22] D. Wang, H.L. Xin, R. Hovden, H. Wang, Y. Yu, D.A. Muller, F.J. DiSalvo, H.D. Abruna, Nat. Mater. 12 (2013) 81.
[23] J.D. Rocca, D. Liu, W. Lin, Acc. Chem. Res. 44 (2011) 957.
[24] D. Ling, T. Hyeon, Small 9 (2013) 1450.
[25] T. Deng, F. Marlow, Chem. Mater. 24 (2012) 536.
[26] S. Wang, M. Zhang, W. Zhang, ACS Catal. 1 (2011) 207.
[27] W. Stober, A. Fink, E.J. Bohn, J. Colloid Interface Sci. 26 (1968) 62.
[28] C. Horváth, S.R. Lipsky, J. Chromatogr. Sci. 7 (1969) 109.
[29] J.J. Kirkland, Anal. Chem. 64 (1992) 1239.
[30] J.J. Kirkland, F.A. Truszkowski, C.H. Dilks Jr., G.S. Engel, J. Chromatogr. A 890 (2000) 3.
[31] F. Honda, H. Honda, M. Koishi, J. Chromatogr. 609 (1992) 49.
[32] H. Honda, M. Kimura, F. Honda, T. Matsuno, M. Koishi, Colloids Surf. A 82 (1994) 117.
[33] F. Honda, H. Honda, M. Koishi, T. Matsuno, J. Chromatogr. A 775 (1997) 13.
[34] W. Tong, X. Song, C. Cao, Chem. Soc. Rev. 41 (2012) 6103.
[35] J.J. Kirkland, T.J. Langlois, US Patent 2009/0297853 A1.
[36] F. Gritti, I. Leonardis, J. Abia, G. Guiochon, J. Chromatogr. A 1217 (2010) 3819.
[37] S. Fekete, D. Guillarme, J. Chromatogr. A 1308 (2013) 104.
[38] A.C. Sanchez, G. Friedlander, S. Fekete, J. Anspach, D. Guillarme, M. Chitty, T. Farkas, J. Chromatogr. A 1311 (2013) 90.
[39] X. Wu, L. You, B. Di, W. Hao, M. Su, Y. Gu, L. Shen, J. Chromatogr. A 1299 (2013) 78.
[40] S.A. Schuster, B.E. Boyes, B.M. Wagner, J.J. Kirkland, J. Chromatogr. A 1228 (2012) 232.
[41] S.A. Schuster, B.M. Wagner, B.E. Boyes, J.J. Kirkland, J. Chromatogr. A 1315 (2013) 118.
[42] M. Spasova, V. Salgueirino-Maceira, A. Schlachter, M. Hilgendorff, M. Giersig, L.M. Liz-Marzan, M. Farle, J. Mater. Chem. 15 (2005) 2095.
[43] H. Dong, J.D. Brennan, Chem. Commun. 47 (2011) 1207.
[44] C. Paek, Y. Huang, M.R. Filgueira, A.V. McCormick, P.W. Carr, J. Chromatogr. A 1229 (2012) 129.
[45] K. Lomsadze, G. Jibuti, T. Farkas, B. Chankvetadze, J. Chromatogr. A 1234 (2012) 50.
[46] J. Moraes, K. Ohno, T. Maschmeyer, S. Perrier, Chem. Mater. 25 (2013) 3522.
[47] G.L. Li, H. Möhwald, D.G. Shchukin, Chem. Soc. Rev. 42 (2013) 3628.
[48] S. Sorribas, B. Zornoza, C. Téllez, J. Coronas, Chem. Commun. 48 (2012) 9388.
[49] A. Ahmed, M. Forster, R. Clowes, D. Bradshaw, P. Myers, H. Zhang, J. Mater. Chem. A 1 (2013) 3276.
[50] J.Y. Sun, Z.K. Wang, H.S. Lim, S.C. Ng, M.H. Kuok, T.T. Tran, X. Liu, ACS Nano 4 (2010) 7692.
[51] A. Ahmed, R. Clowes, E. Willneff, H. Ritchie, P. Myers, H. Zhang, Ind. Eng. Chem. Res. 49 (2010) 602.
[52] S. Wu, C. Mou, H. Lin, Chem. Soc. Rev. 42 (2013) 3862.
[53] C. Graf, D.L.J. Vossen, A. Imhof, A. van Blaaderen, Langmuir 19 (2003) 6693.
[54] W. Li, D. Zhao, Adv. Mater. 25 (2013) 142.
[55] G. Büchel, K.K. Unger, A. Matsumoto, K. Tsutsumi, Adv. Mater. 10 (1998) 1036.
[56] Y. Deng, D. Qi, C. Deng, X. Zhang, D. Zhao, J. Am. Chem. Soc. 130 (2008) 28.
[57] J. Li, W. Ma, C. Wei, J. Guo, J. Hu, C. Wang, J. Mater. Chem. 21 (2011) 5992.
[58] M. Shao, F. Ning, J. Zhao, M. Wei, D.G. Evans, X. Duan, J. Am. Chem. Soc. 134 (2012) 1071.
[59] F. Hu, S. Chen, R. Yuan, Sens. Actuators B 176 (2013) 713.
[60] H. Chen, C. Deng, X. Zhang, Angew. Chem. Int. Ed. 49 (2010) 607.
[61] L. Han, H. Wei, B. Tu, D. Zhao, Chem. Commun. 47 (2011) 8536.
[62] A.B. Fuertes, P. Valle-Vigón, M. Sevilla, Chem. Commun. 48 (2012) 6124.
[63] A. Ahmed, H. Ritchie, P. Myers, H. Zhang, Adv. Mater. 24 (2012) 6042.
[64] A. Ahmed, W. Abdelmagid, H. Ritchie, P. Myers, H. Zhang, J. Chromatogr. A 1270 (2012) 194.
[65] H.-C. Zhou, J.R. Long, O.M. Yaghi, Chem. Rev. 112 (2012) 673.
[66] K.A. Cychosz, R. Ahmad, A.J. Matzger, Chem. Sci. 1 (2010) 293.
[67] Z.Y. Gu, C. Yang, N. Chang, X.P. Yan, Acc. Chem. Res. 45 (2012) 734.
[68] Y.Y. Fu, C.X. Yang, X.P. Yang, Chem. Eng. J. 19 (2013) 13484.
[69] W. Wang, M. Zhang, L. Chu, Acc. Chem. Res. 47 (2014) 373.
[70] J.I. Park, A. Saffari, S. Kumar, A. Günther, E. Kumacheva, Annu. Rev. Mater. Res. 40 (2010) 415.
[71] J. Wang, J. Wang, J. Han, Small 7 (2011) 1728.
[72] J.H. Kim, T.Y. Jeon, T.M. Choi, T.S. Shim, S.H. Kim, S.M. Yang, Langmuir 30 (2014) 1473.
[73] Z. Nie, J.I. Park, W. Li, S.A.F. Bon, E. Kumacheva, J. Am. Chem. Soc. 130 (2008) 16508.
[74] J. Wu, T. Kong, K.W.K. Yeung, H.C. Shum, K.M.C. Cheung, L. Wang, M.K.T. To, Acta Biomater. 9 (2013) 7410.
[75] W. Lan, S. Li, J. Xu, G. Luo, Langmuir 27 (2011) 13242.
[76] C. Zhao, A.P.J. Middelberg, RSC Adv. 3 (2013) 21227.
[77] J.H. Knox, J. Chromatogr. A 831 (1999) 3.
[78] F. Gritti, T. Farkas, J. Heng, G. Guiochon, J. Chromatogr. A 1218 (2011) 8209.
[79] F. Gritti, G. Guiochon, J. Chromatogr. A 1218 (2011) 3476.
[80] J.C.M. Garnett, Philos. Trans. R. Soc. London Ser. B 203 (1904) 385.
[81] S. Torquato, Random Heterogeneous Materials: Microstructure and Macroscopic Properties, Springer, New York, NY, 2002.
[82] S. Torquato, J. Appl. Phys. 58 (1985) 3790.
[83] F. Gritti, G. Guiochon, Chem. Eng. Sci. 66 (2011) 3773.
[84] J.H. Knox, H.P. Scott, J. Chromatogr. 282 (1983) 297.
[85] F. Gritti, Chromatogr. Today May/June (2012) 4.
[86] Guiochon, J. Chromatogr. A 1168 (2007) 101.
[87] Minakuchi, K. Nakanishi, N. Soga, N. Ishizuka, N. Tanaka, Anal. Chem. 68 (1996) 3498.
[88] K.S. Mriziq, J.A. Abia, Y. Lee, G. Guiochon, J. Chromatogr. A 1193 (2008) 97.
[89] N. Vervoort, P. Gzill, G.V. Baron, G. Desmet, J. Chromatogr. A 1030 (2004) 177.
[90] K. Cabrera, J. Sep. Sci. 27 (2004) 843.
[91] F.C. Leinweber, D. Lubda, K. Cabrera, U. Tallarek, Anal. Chem. 74 (2002) 2470.
[92] A. Soliven, D. Foley, L. Pereira, G.R. Dennis, R.A. Shalliker, K. Cabrera, H. Ritchie, T. Edge, J. Chromatogr. A 1334 (2014) 16.
[93] K. Hormann, T. Müllner, S. Bruns, A. Höltzel, U. Tallarek, J. Chromatogr. A 1222 (2012) 46.
[94] D. Cabooter, K. Broeckhoven, R. Sterken, A. Vanmessen, I. Vandendael, K. Nakanishi, S. Deridder, G. Desmet, J. Chromatogr. A 1325 (2014) 72.
[95] M. Camenzuli, H.J. Ritchie, J.R. Ladine, R.A. Shalliker, Analyst 136 (2011) 5127.
[96] F. Gritti, G. Guiochon, J. Chromatogr. A 1297 (2013) 64.
[97] D. Kocic, L. Pereira, D. Foley, T. Edge, J. Mosely, H. Ritchie, X. Conlan, R.A. Shalliker, J. Chromatogr. A 1305 (2013) 102.
[98] D. Foley, L. Pereira, M. Camenzuli, T. Edge, H. Ritchie, R.A. Shalliker, Microchem. J. 110 (2013) 127.
[99] P.C. Carman, Trans. Inst. Chem. Eng. 15 (1937) 150.
[100] H. Poppe, J. Chromatogr. A 778 (1997) 3.
[101] G. Desmet, D. Clicq, P. Gzil, Anal. Chem. 77 (2005) 4058.
[102] G. Desmet, D. Clicq, D.T.-T. Nguyen, D. Guillarme, S. Rudaz, J.-L. Veuthey, N. Vervoort, G. Torok, D. Cabooter, P. Gzil, Anal. Chem. 78 (2006) 2150.
[103] J.H. Knox, P.A. Bristow, Chromatographia 10 (1977) 279.
[104] J.J. DeStefano, T.J. Langlois, J.J. Kirkland, J. Chromatogr. Sci. 46 (2008) 254.
[105] J.J. Kirkland, T.J. Langlois, J. DeStefano, J. Am. Lab. 39 (2007) 18.
[106] K. Kaczmarski, G. Guiochon, Anal. Chem. 79 (2007) 4648.

[107] N. Marchetti, G. Guiochon, J. Chromatogr. A 1176 (2007) 206.
[108] N. Marchetti, A. Cavazzini, F. Gritti, G. Guiochon, J. Chromatogr. A 1163 (2007) 203.
[109] F. Gritti, G. Guiochon, J. Chromatogr. A 1217 (2010) 1604.
[110] F. Gritti, I. Leonardis, D. Shock, P. Stevenson, A. Shalliker, G. Guiochon, J. Chromatogr. A 1217 (2010) 1589.
[111] E. Oláh, S. Fekete, J. Fekete, K. Ganzler, J. Chromatogr. A 1217 (2010) 3642.
[112] B.M. Wagner, S.A. Schuster, B.E. Boyes, J.J. Kirkland, J. Chromatogr. A 1264 (2012) 22.
[113] T. Taneuchi, Anal. Bioanal. Chem. 375 (2003) 25.
[114] T. Taneuchi, Chromatography 26 (2005) 1.
[115] S. Bruns, J.P. Grinias, L.E. Blue, J.W. Jorgenson, U. Tallarek, Anal. Chem. 84 (2012) 4496.
[116] R.G. Avery, J.D. Ramsay, J. Colloid Interface Sci. 42 (1973) 597.
[117] L.A. Colon, T.D. Maloney, A.M. Fermier, J. Chromatogr. A 887 (2000) 43.
[118] R.J. Boughtflower, T. Underwood, C.J. Paterson, Chromatographia 40 (1995) 329.
[119] A.M. Fermier, L. Colon, J. Microcolumn Sep. 10 (1998) 439.
[120] P. Marhol, R. Gazak, P. Badnar, V. Kren, J. Sep. Sci. 34 (2011) 2206.
[121] J.O. Omamogho, J.D. Glennon, Anal. Chem. 83 (2011) 1547.
[122] F. Gritti, G. Guiochon, J. Chromatogr. A 1333 (2014) 60.
[123] F. Fanali, A. Rocco, Z. Aturki, L. Mondello, S. Famali, J. Chromatogr. A 1234 (2012) 38.
[124] S. Fanali, S. Rocchi, B. Chankvetadze, Electrophoresis 34 (2013) 1737.
[125] A.J. Alpert, J. Chromatogr. 499 (1990) 177.
[126] J. Pesek, M.T. Matyska, LC-GC 25 (2007) 480.
[127] J.J. Kirkland, S.A. Schuster, W.L. Johnson, B.E. Boyes, J. Pharm. Anal. 3 (2013) 303.
[128] B. Chauve, D. Guillarme, P. Cleon, J.L. Veuthey, J. Sep. Sci. 33 (2010) 752.
[129] T.A. Berger, J. Chromatogr. A 1218 (2011) 4559.
[130] A. Cavazzini, L. Pasti, A. Massi, N. Marchetti, F. Dondi, Anal. Chim. Acta 706 (2011) 205.
[131] E. Yashima, J. Chromatogr. A 906 (2001) 105.
[132] X. Lai, W. Tang, S.C. Ng, J. Chromatogr. A 1218 (2011) 5597.
[133] T.J. Ward, K.D. Ward, Anal. Chem. 84 (2012) 626.
[134] M.G. Cikalo, K.D. Bartle, M.M. Robson, P. Myers, M.R. Euerby, Analyst 123 (1998) 87R.
[135] D. Wistuba, J. Chromatogr. A 1217 (2010) 941.
[136] H. Lu, G. Chen, Anal. Methods 3 (2011) 488.
[137] S. Fanali, G. D'Orazio, T. Farkas, B. Chankvetadze, J. Chromatogr. A 1269 (2012) 136.
[138] D.R. Stoll, X. Li, X. Wang, P.W. Carr, S.E.G. Porter, S.C. Rutan, J. Chromatogr. A 1168 (2007) 3.
[139] J.N. Fairchild, K. Horváth, G. Guiochon, J. Chromatogr. A 1216 (2009) 1363.
[140] D.R. Stoll, X. Wang, P.W. Carr, Anal. Chem. 80 (2008) 268.
[141] A.J. Alexander, L. Ma, J. Chromatogr. A 1216 (2009) 1338.
[142] S. Kittlaus, J. Schimanke, G. Kempe, K. Speer, J. Chromatogr. A 1283 (2013) 98.
[143] S.A. Schuster, B.M. Wagner, B.E. Boyes, J.J. Kirkland, J. Chromatogr. Sci. 48 (2010) 566.
[144] S. Fekete, R. Berky, J. Fekete, J.-L. Veuthey, D. Guillarme, J. Chromatogr. A 1236 (2012) 177.
[145] A. Staub, D. Zurlino, S. Rudaz, J.-L. Veuthey, D. Guillarme, J. Chromatogr. A 1218 (2011) 8903.
[146] J. Ruta, D. Zurlino, C. Grivel, S. Heinisch, J.-L. Veuthey, D. Guillarme, J. Chromatogr. A 1228 (2012) 221.
[147] S. Fekete, D. Guillarme, J. Chromatogr. A 1320 (2013) 86.
[148] A. Martínez-Villalba, E. Moyano, C.B. Martins, M. Galceran, Anal. Bioanal. Chem. 397 (2010) 2893.
[149] Á. Tölgyesi, V.K. Sharma, J. Fekete, J. Chromatogr. B 879 (2011) 403.
[150] Y. Lu, Q. Shen, Z. Dai, H. Zhang, Anal. Bioanal. Chem. 398 (2010) 1819.
[151] D. Šatínský, K. Jägerová, L. Havlíková, P. Solich, Food Anal. Methods 6 (2013) 1353.
[152] K.P. Yáñez, J.L. Bernal, M.J. Nozal, M.T. Martín, J. Bernal, J. Chromatogr. A 1285 (2013) 110.
[153] H. Gallart-Ayala, O. Núñez, P. Lucci, Trends Anal. Chem. 42 (2013) 99.
[154] H. Gallart-Ayala, E. Moyano, M.T. Galceran, J. Chromatogr. A 1218 (2011) 1603.
[155] H. Gallart-Ayala, E. Moyano, M.T. Galceran, Anal. Chim. Acta 683 (2011) 227.
[156] S. Bayen, X. Yi, E. Segovia, Z. Zhou, B.C. Kelly, J. Chromatogr. A 1338 (2014) 38.
[157] P. Vazquez-Roig, C. Blasco, Y. Picó, Trends Anal. Chem. 50 (2013) 65.
[158] N. Fontanals, R.M. Marcé, F. Borrull, J. Chromatogr. A 1218 (2011) 5975.
[159] M. Pedrouzo, F. Borrull, E. Pocurull, R.M. Marcé, J. Sep. Sci. 34 (2011) 1091.
[160] L. Ciofi, D. Fibbi, U. Chiuminatto, E. Coppini, L. Checchini, M. Del Bubba, J. Chromatogr. A 1283 (2013) 53.
[161] H. Gallart-Ayala, E. Moyano, M.T. Galceran, J. Chromatogr. A 1217 (2010) 3511.
[162] W. Peysson, E. Vulliet, J. Chromatogr. A 1290 (2013) 46.
[163] M.C. Hurtado-Sánchez, R. Romero-González, M.I. Rodríguez-Cáceres, I. Durán-Merás, A.G. Frenich, J. Chromatogr. A 1305 (2013) 193.
[164] P. Zhang, A. Bui, G. Rose, G. Allinson, J. Chromatogr. A 1325 (2014) 56.
[165] P. Chocholouš, J. Vacková, I. Šrámková, D. Šatínský, P. Solich, Talanta 103 (2013) 221.
[166] G. Vinci, M.L. Antonelli, R. Preti, J. Sep. Sci. 36 (2013) 461.
[167] G. Purcaro, S. Moret, M. Bučar-Miklavčič, L.S. Conte, J. Sep. Sci. 35 (2012) 922.